Drug-Induced Alterations of Mitochondrial DNA Homeostasis in Steatotic and Nonsteatotic HepaRG Cells

Dounia Le Guillou, Simon Bucher, Karima Begriche, Delphine Hoët, Anne Lombès, Gilles Labbe, Bernard Fromenty

Title:

Drug-induced alterations of mitochondrial DNA homeostasis in steatotic and non-steatotic HepaRG cells

Authors:

Dounia Le Guillou, Simon Bucher, Karima Begriche, Delphine Hoët, Anne Lombès, Gilles Labbe, Bernard Fromenty

Primary laboratory of origin:

INSERM, INRA, Univ Rennes, UBL, Nutrition Metabolisms and Cancer (NuMeCan), Rennes, France

Affiliations:

DLG, SB, KB, BF: INSERM, INRA, Univ Rennes, UBL, Nutrition Metabolisms and Cancer (NuMeCan), Rennes, France

DH, GL: Sanofi, Investigative Toxicology, 94140 Alfortville, France

AL : Inserm, UMR 1016, Institut Cochin, Université Paris V René Descartes, Paris, France

Running title:

Drug-induced alterations of mitochondrial DNA homeostasis

Corresponding Author:

Bernard Fromenty

INSERM**,** UMR 1241, Université de Rennes 1, 35000 Rennes, France

Phone number: (+33)2 23 23 30 44, Fax number: (+33)2 23 23 64 64

E-mail address: bernard.fromenty@inserm.fr

Number of text pages: 29

Number of tables: 4

Number of figures: 7

Number of references: 59

Number of words in the Abstract: 250

Number of words in the Introduction: 628

Number of words in the Discussion: 1475

Abbreviations: AMPKα: AMP-activated protein kinase α-subunit; APOA4: apolipoprotein A4; COX2: cytochrome *c* oxidase subunit 2 (protein); COX4: cytochrome *c* oxidase subunit 4 (protein); COX4I1: cytochrome *c* oxidase subunit 4 (gene); CS: citrate synthase; CYP: cytochrome P450; ddC: zalcitabine; FAO: fatty acid oxidation; IC_{10}: 10% inhibitory concentration; IC_{50}: 50% inhibitory concentration; LNZ: linezolid; MT-CO2: cytochrome *c* oxidase subunit 2 (gene); mtDNA: mitochondrial DNA; MT-ND1: NADH dehydrogenase subunit 1 (gene); NAFLD; nonalcoholic fatty liver disease; ND1: NADH dehydrogenase subunit 1 (protein); nDNA: nuclear DNA; NFE2L2: nuclear factor erythroid 2-like 2; NRF: nuclear respiratory factor; NRTI: nucleoside reverse transcriptase inhibitor; OXPHOS: oxidative phosphorylation; PBS: phosphate buffer saline; PGC-1: peroxisome proliferator-activated receptor-γ coactivator 1; PI: protease inhibitor; PLIN: perilipin; POLG: DNA polymerase γ; POLRMT: mitochondrial RNA polymerase; TFAM: mitochondrial transcription factor A

Recommended section assignment: Toxicology

Abstract

Although mitochondriotoxicity plays a major role in drug-induced hepatotoxicity, alteration of mitochondrial DNA (mtDNA) homeostasis has been described only with a few drugs. Because it requires long drug exposure, this mechanism of toxicity cannot be detected with investigations performed in isolated liver mitochondria or cultured cells exposed to drugs for several hours, or a few days. Thus, a first aim of this study was to determine whether a 2-week treatment with 9 hepatotoxic drugs could affect mtDNA homeostasis in HepaRG cells. Previous investigations with these drugs showed rapid toxicity on oxidative phosphorylation but did not address the possibility of delayed toxicity secondary to mtDNA homeostasis impairment. The maximal concentration used for each drug induced about 10% cytotoxicity. Two other drugs, zalcitabine and linezolid, were used as positive controls for their respective effects on mtDNA replication and translation. Another goal was to determine whether drug-induced mitochondriotoxicity could be modulated by lipid overload mimicking nonalcoholic fatty liver. Among the 9 drugs, imipramine and ritonavir induced mitochondrial effects suggesting alteration of mtDNA translation. Ritonavir toxicity was stronger in non-steatotic cells. None of the 9 drugs decreased mtDNA levels. However, increased mtDNA was observed with 5 drugs, especially in non-steatotic cells. mtDNA levels could not be correlated with the expression of key factors involved in mitochondrial biogenesis (e.g. PGC1α, PGC1β, AMPKα). Hence, drug-induced impairment of mtDNA translation might not be rare and increased mtDNA levels could be a frequent adaptive response to slight energy shortage. Nevertheless, this adaptation could be impaired by lipid overload.

Introduction

Although mitochondrial dysfunction is deemed to be a major mechanism of drug-induced liver injury (DILI) (Begriche et al., 2011; Will and Dykens, 2014), alteration of mitochondrial DNA (mtDNA) homeostasis has been described so far only with a few drugs (Cohen, 2010; Schon and Fromenty, 2016). For instance, the antiretroviral nucleoside reverse transcriptase inhibitors (NRTIs) zalcitabine (ddC), stavudine (d4T) and zidovudine (AZT) are able to block mtDNA replication via an inhibition of the DNA polymerase γ, thus inducing a progressive reduction of mtDNA levels in liver (Walker et al., 2004; Schon and Fromenty, 2016). The antibiotics linezolid (LNZ) and tetracycline can specifically impair mtDNA translation, possibly by interacting with the mitochondrial ribosomes (De Vriese et al., 2006; Moullan et al., 2015).

Because mtDNA encodes for 13 oxidative phosphorylation (OXPHOS) polypeptides, any significant alteration of mtDNA replication, transcription or translation can cause energy shortage and severe liver diseases (Wallace et al., 2010; Schon and Fromenty, 2016). However, because there is an excess of mtDNA copies in most cells, OXPHOS will be impaired only after severe decrease of the mtDNA content (Schon and Fromenty, 2016). It is deemed that the number of mtDNA copies must fall below 20-40% of basal levels in order to induce a significant mitochondrial dysfunction (Igoudjil et al., 2006; Begriche et al., 2011). Importantly, other threshold effects exist in mitochondria including at the levels of mitochondrial protein synthesis and OXPHOS activity (Rossignol et al., 1999; Rossignol et al., 2003). These different thresholds explain why mitochondrial toxicity and liver injury induced by NRTIs and LNZ can occur in patients after several weeks or months of treatment (Spengler et al., 2002; Walker et al., 2004; De Vriese et al., 2006; De Bus et al., 2010).

Currently, most in vitro investigations addressing drug-induced mitochondrial toxicity are performed in isolated liver mitochondria (Porceddu et al., 2012; Marroquin et al., 2014) and in cultured cells exposed to the tested drugs for several hours, or a few days at the most (Kamalian et al., 2015; Eakins et al., 2016). These investigations can detect direct and rapid impairment of OXPHOS and fatty acid oxidation (FAO) pathway but not mitochondrial dysfunction secondary to alterations of mtDNA homeostasis.

Hence, a first aim of this study was to investigate, in the metabolically competent human hepatoma HepaRG cell line, the effects of 11 hepatotoxic drugs on mtDNA homeostasis after 2 weeks of treatment, namely LNZ, ddC, amiodarone, atorvastatin, carbamazepine, imipramine, lovastatin, perhexiline, ritonavir, terbinafine and troglitazone. The drugs ddC and LNZ were selected as model molecules to ascertain that HepaRG cells could be used as a valuable model to detect drug-induced inhibition of mtDNA replication and translation, respectively (Walker et al., 2004; De Vriese et al., 2006; Schon and Fromenty, 2016). The other drugs were chosen because previous studies in isolated liver mitochondria showed that they directly impaired OXPHOS at relatively low concentrations (Fromenty et al., 1990; Deschamps et al., 1994; Porceddu et al., 2012) but these investigations did not address the possibility that their hepatotoxicity might also be mediated by a deleterious effect on mtDNA homeostasis.

The second aim of this study was to compare the long-term cytotoxicity and mitochondriotoxicity of these drugs between non-steatotic and steatotic HepaRG cells. Indeed, some drugs such as acetaminophen, halothane and methotrexate are more hepatotoxic in the context of obesity and associated nonalcoholic fatty liver disease (NAFLD) (Fromenty, 2013; Michaut et al., 2014; Massart et al., 2017). Although the mechanisms of this increased susceptibility are not precisely known, higher formation of cytochrome P450 (CYP)-generated toxic metabolites and preexistent mitochondrial dysfunction could be involved, at least for some pharmaceuticals (Fromenty, 2013; Massart et al., 2017). Because obesity and NAFLD are highly prevalent in numerous countries, it is important to determine which drugs could present a higher risk of hepatotoxicity in obese patients.

Materials and Methods

Chemicals and reagents

Amiodarone, atorvastatin, carbamazepine, imipramine, lovastatin, perhexiline, ritonavir, terbinafine, troglitazone, ddC, LNZ, testosterone, 6β-hydroxytestosterone, chlorzoxazone (CZX), dimethyl sulfoxide (DMSO), D-(+)-galactose, oleic acid, stearic acid and insulin were purchased from Sigma Aldrich (Saint-Quentin-Fallavier, France). [U-^{14}C]-palmitic acid was supplied by PerkinElmer (Waltham, MA). A-769662 was purchased from Santa Cruz (Santa Cruz, CA). William's E medium, glutamine, penicillin/streptomycin, Nile red and Hoechst dyes were obtained from Thermo Fischer Scientific (Waltham, MA). William's E medium without glucose was supplied by CliniSciences (Nanterre, France). Fetal Bovine Serum (FBS) was supplied by Lonza (Levallois-Perret, France). Hydrocortisone hemisuccinate was purchased from SERB Laboratories (Paris, France). Protease and phosphatase inhibitors were supplied by Roche Diagnostics (Indianapolis, IN).

Cell cultures and treatments

Native HepaRG cells were cultured as previously described (Michaut et al., 2016). Briefly, HepaRG cells were seeded at a density of 2.6 x 10^4 cells/cm^2 and were first incubated in a William's E medium supplemented with 10% FBS, 100 units/ml penicillin, 100 µg/ml streptomycin, 2 mM glutamine, 5 µg/ml insulin and 50 µM hydrocortisone hemisuccinate. After 2 weeks, cell differentiation was induced by culturing the HepaRG cells in the same medium supplemented with 2% DMSO for 2 additional weeks. Cells were then maintained for 2 additional weeks in the same culture medium except for the FBS and DMSO concentrations that were set at 5 and 1%, respectively. In order to induce steatosis, HepaRG cells were treated during this 2 week-period with a mixture of stearic acid (150 µM) and oleic acid (150 µM). For drug treatments, non-steatotic and steatotic HepaRG cells were incubated during the same period with each compound at different concentrations. In some experiments, cells were treated with 30 µM of A-769662, a direct activator of AMP-activated protein kinase α-subunit (AMPKα) (Smith et al., 2016). Stearic acid, oleic acid and the different drugs were dissolved in DMSO whose final concentration in

cultures was always maintained at 1%. Whatever the treatments including A-769662, the culture medium was renewed every 2 or 3 days during the 2-week experiments. To this end, newly added medium contained each selected drug (or no drug) with or without the fatty acid mixture. For some investigations with LNZ, ddC, imipramine and ritonavir, HepaRG cells were treated for 3 days with two treatments over this time period. All investigations were performed 24 h after the last drug treatment, excepted for AMPKα activation that was assessed 6 h after the last drug treatment. HepaRG cells were used at passages 11 to 15.

Primary human hepatocytes (PHH) were obtained from Biopredic International (Saint-Grégoire, France). Briefly, PHH were isolated by collagenase perfusion of peritumoral liver tissue from 4 male adult donors who underwent resection for hepatic metastases. PHH were then seeded at a density of 0.2×10^5 cells/cm^2 onto rat collagen I-coated plates in a medium provided by Biopredic International. This medium was discarded 12 h after cell seeding and PHH cultures were maintained for 24 h in William's E medium supplemented with 10% FBS, 2 % DMSO, 100 units/ml penicillin, 100 µg/ml streptomycin, 2 mM glutamine, 5 µg/ml insulin and 50 µM hydrocortisone hemisuccinate. PHH were then maintained for 12 days in the same culture medium except for the FBS and DMSO concentrations that were set at 5 and 1%, respectively. PHH were treated or not for 12 days with fatty acids and drugs using the same protocol as for HepaRG cells.

Nile red staining, cellular triglycerides and cytotoxicity assays

The Nile red dye allows the staining of neutral lipids within cells. For Nile red staining, cells were washed with warm phosphate buffer saline (PBS), fixed with 4% paraformaldehyde for 20 min at room temperature and then washed three times with cold PBS. After paraformaldehyde fixation, cells were incubated with 0.05 µg/ml Nile red in PBS for 30 min at room temperature and then washed once with PBS. Nuclei were labelled with 10 µg/ml Hoechst dye and cells were observed with an ImageXpress Micro Confocal High-Content Imaging System (Molecular Devices, Berkshire, UK). Triglycerides were measured with a colorimetric kit purchased from Biovision (Milpitas, CA), using the manufacturer's recommendations. Cytotoxicity was assessed by measuring cellular ATP levels using the CellTiter-Glo Luminescent Cell Viability assay purchased from Promega (Charbonnières, France), according to the manufacturer's instructions. Briefly, untreated and treated HepaRG cells were first incubated with the CellTiter-Glo reagent

for 10 min at 37°C. Cells were then transferred in an opaque-walled multiwell plate and the luminescent signal was quantified using a POLARstar Omega microplate reader (BMG Labtech, Ortenberg, Germany). Results were expressed in comparison to untreated cells. Fifty and 10% inhibitory concentration (IC_{50} and IC_{10}) values were calculated with a 4-parameter logistic regression using GraphPad Prism software 6.0 (GraphPad, San Diego, CA).

Determination of CYP2E1 and CYP3A4 activities

Measurement of CYP2E1 and CYP3A4 activities was performed as recently described (Michaut et al., 2016). Briefly, HepaRG cells were incubated for 6 and 2 h in phenol red-free and DMSO-free William's E medium containing 300 µM CZX or 200 µM testosterone, respectively. At the end of the incubation, cell culture media were collected and stored at -80°C until analysis. 6-Hydroxychlorzoxazone was then quantified by high-performance liquid chromatography (HPLC)-tandem mass spectrometry (Xenoblis, Rennes, France), whereas 6β-hydroxytestosterone was measured by HPLC analysis.

Assessment of mtDNA levels

Total DNA was extracted from about $3x10^5$ HepaRG cells using a Blood and Cell Culture DNA Mini Kit (Qiagen, Les Ulis, France). The relative content of mtDNA was then assessed by real-time quantitative PCR analysis (RT-qPCR) using the SYBR Green PCR Master Mix (Applied Biosystem, Woolston, UK) and an Applied Biosystem 7900HT Fast Real-Time PCR System (Applied Biosystem). The primers used to amplify a portion of the mtDNA gene encoding the cytochrome *c* oxidase subunit 1 (MT-CO1, also referred to as COX1) were 5'-TACGTTGTAGCCCACTTCCACT-3' (forward) and 5'-AGTAACGTCGGGGCATTCCG-3' (reverse). For normalization of mtDNA content, a portion of the nDNA gene encoding the ribosomal protein S6 (RPS6) was amplified by using the following primers 5'-TGATGTCCGCCAGTATGTTG-3' (forward) and 5'-TCTTGGTACGCTGCTTCTTC-3' (reverse). The $2^{-\Delta\Delta Ct}$ method was then used to assess the relative mtDNA levels.

Isolation of RNA and measurement of gene expression

Total RNA was extracted from about $6x10^5$ HepaRG cells with the Nucleospin RNA isolation system purchased from Macherey-Nagel (Hoerdt, France), which included a DNase treatment step. RNAs were reverse-transcribed into cDNAs using the High-Capacity cDNA Reverse Transcription Kit purchased from Applied Biosystems. RT-qPCR was then performed as mentioned above. Expression of GAPDH was used as reference, and the $2^{-\Delta\Delta Ct}$ method was used to express the relative expression of each selected gene. The sequences of the primers used to measure gene expression are presented in the Table 1.

Western blot analysis

At the end of the treatments, cells were harvested, washed twice with ice-cold PBS and lysed in a RIPA buffer (150 mM NaCl, 50 mM Tris-HCl pH 7.4, 0.25% sodium deoxycholate, 0.1% sodium dodecylsulfate, 1 mM EDTA, 1% NP-40) supplemented with protease and phosphatase inhibitors. Twenty µg of proteins were then separated by electrophoresis on NuPAGE 4-12% gradient Bis-Tris gels (Thermo Fisher Scientific), transferred to 0.2-µm nitrocellulose membranes (Bio-Rad, Hercules, CA), which were saturated with 5% bovine serum albumin (BSA) in Tris-buffered saline (TBS) containing 0.1% Tween 20 (TBS-T) for 2 h at room temperature. Proteins were then immunoblotted with antibodies against NADH dehydrogenase subunit 1 (ND1), cytochrome *c* oxidase subunits 2 and 4 (COX2 and COX4), mitochondrial ribosomal protein L11 (MRPL11), MRPL28, AMP-activated protein kinase α-subunit (AMPKα), phospho-AMPKα and β-actin, which was used as loading control. The dilution used for all antibodies was 1:1000 except for those against COX2 and β-actin whose dilutions were 1:500 and 1:5000 respectively. Finally, blots were incubated with appropriate secondary antibodies, and protein bands were revealed by enhanced chemiluminescence with the Fusion-FX7 Spectra system (Vilber Lourmat, Eberhardzell, Germany). COX4 and MRPL28 antibodies were purchased from Abcam (Cambridge, UK). AMPKα, phospho-AMPKα (Thr172) and MRPL11 antibodies were purchased from Cell Signaling (Danvers, MA). β-Actin antibodies were purchased from Santa Cruz Biotechnology (Dallas, TX). ND1 and COX2 antibodies were generated by the group of Dr Anne Lombès, as previously reported (Agier et al., 2012).

Measurement of citrate synthase activity and respiratory chain complex I levels and activity

Citrate synthase (CS) activity was measured with 20 µg of proteins using the Citrate Synthase Assay Kit from Sigma-Aldrich, according to the manufacturer recommendations. Complex I levels and activity were respectively measured with the Complex I Human Protein Quantity Dipstick Assay Kit and the Complex I Enzyme Activity Dipstick Assay kit purchased from Abcam, according to the manufacturer instructions. In the assay, complex I is immunocaptured and immuno-precipitated in active form on the dipstick that consists of a nitrocellulose membrane to which an anti-complex I monoclonal antibody is attached. Complex I levels and activity were measured immunochromatographically with 20 µg of proteins using a Hamamatsu MS1000 Dipstick Reader (Abcam).

Measurement of mitochondrial respiration and fatty acid oxidation

Mitochondrial respiration in the presence of L-glutamine (2 mM), glucose (10 mM) and pyruvate (1 mM) was measured in adherent HepaRG cells using an Agilent Seahorse XFe24 Analyzer and the Mito Stress Test Kit (Agilent, Santa Clara, CA), according to the manufacturer instructions. Oxygen consumption rates were normalized in each well by the number of cells estimated by the fluorescence intensity of the Hoechst dye (10 µg/ml). For some investigations, HepaRG cells were also cultured in a William's E medium without glucose but supplemented with 11.1 mM galactose. After 14 days, mitochondrial respiration was measured for each culture condition (i.e. glucose or galactose) in the presence of L-glutamine/pyruvate/glucose or L-glutamine/pyruvate/galactose with glucose and galactose at the same concentration (i.e. 10 mM). These experiments showed that HepaRG cells cultured for 14 days with glucose or galactose presented similar basal and maximal (i.e. FCCP-stimulated) mitochondrial respiration measured in the presence of glucose (Table 2). A trend towards lower maximal respiration was noticed when mitochondrial respiration was measured in the presence of galactose (Table 2). The ATP production parameter was similar between the different conditions (Table 2). Non-mitochondrial respiration and proton leak (two other parameters provided by the Mito Stress Test profile) were also unchanged between the 4 different conditions of mitochondrial assessment (data not shown). Mitochondrial fatty acid oxidation (FAO) was measured in adherent HepaRG cells using [U-^{14}C]palmitic acid (0.05 µCi/ml), as previously described (Anthérieu et al., 2011). Results for mitochondrial FAO were normalized to the total protein content determined by the bicinchoninic acid method.

Statistical analysis

All results are expressed as mean ± SEM (standard error of mean). Comparisons between two groups were performed with a t-test. Comparisons between multiple groups were performed with two-way analysis of variance (ANOVA). When ANOVA provided significant differences, individual means were compared with the post hoc Bonferroni test. Statistical analyses were performed using GraphPad Prism software 6.0.

Results

Detection of drug-induced alterations of mtDNA homeostasis in HepaRG cells

ddC and LNZ are known inhibitors of mtDNA replication and translation, respectively (Walker et al., 2004; De Vriese et al., 2006; Schon and Fromenty, 2016). In a first series of experiments, we verified that a 2-week treatment with ddC and LNZ could induce these mitochondrial effects in differentiated HepaRG cells. A concentration of 20 μM was used for each drug because our preliminary data showed no significant cytotoxicity that could interfere with the interpretation of the results. ddC strongly reduced mtDNA levels and this was associated with lower mRNA and protein expression of ND1 and COX2, two mtDNA-encoded polypeptides (Fig. 1A, B, C). However, the expression of the nDNA-encoded COX4 was not decreased (Fig. 1C). Complex I levels were significantly reduced by ddC but the activity of this complex was less affected (P=0.15) (Fig. 1D). Regarding LNZ, the 2-week treatment reduced the protein expression of ND1 and COX2, whereas COX4 protein expression, mtDNA levels and mRNA expression of MT-ND1 and MT-CO2 were not decreased (Fig. 1A, B, C). Complex I levels tended to be decreased (P=0.06), while complex I activity was unaffected (Fig. 1D). Finally, HepaRG cells were treated for 72 h with ddC (20 μM) and LNZ (20 μM). No mtDNA depletion was observed with ddC and the protein expression of ND1 and COX2 was not affected by LNZ (data not shown). Our 2-week treatment protocol was therefore appropriate to detect drug-induced impairment of mtDNA replication and translation as well as the functional consequences of these deleterious effects.

Validation of the HepaRG cell as a model of NAFLD

In a recent study carried out in HepaRG cells, we set up a model to study drug-induced hepatotoxicity in the context of NAFLD (Michaut et al., 2016). One rationale of that study was to find optimal conditions of HepaRG cell culture and fatty acid incubation inducing higher CYP2E1 activity and lower CYP3A4 activity, which are both consistent alterations reported in NAFLD patients (Aubert et al., 2011; Woolsey et al., 2015; Michaut et al., 2016). Higher CYP2E1 activity and lower CYP3A4 activity were obtained in HepaRG cells incubated for one week with stearic acid (Michaut et al., 2016). However, incubation of the

HepaRG cells with stearic acid for 2 weeks induced significant toxicity (~15% decrease in cellular ATP levels) leading to modification of the protocol. After testing several conditions of fatty acid incubation, we found that a 2-week treatment with a mixture of stearic acid (150 μM) and oleic acid (150 μM) did not cause significant cytotoxicity (data not shown) and gave satisfying results regarding cellular accumulation of neutral lipids including triglycerides (Fig. 2A), mRNA expression of the lipid biomarkers apolipoprotein A4 (APOA4), perilipin 1 (PLIN1) and perilipin 2 (PLIN2, also known as ADFP) (Fig. 2B). Furthermore, CYP2E1 mRNA expression and activity were increased while CYP3A4 mRNA expression and activity were decreased (Fig. 2B, C). Thus, this protocol of fatty acid treatment was selected for the present study.

Drug-induced cytotoxicity in non-steatotic and steatotic cells

One major goal of this study was to determine whether mtDNA homeostasis could be affected in non-steatotic and steatotic HepaRG cells by different drugs, namely amiodarone, atorvastatin, carbamazepine, imipramine, lovastatin, perhexiline, ritonavir, terbinafine and troglitazone. To this end, preliminary investigations were performed to assess the cytotoxic potential of each drug in order to select non-cytotoxic drug concentrations for further studies on mtDNA homeostasis. Hence, cytotoxicity was determined by treating HepaRG cells with increasing concentrations of each drug and IC_{50} and IC_{10} values were calculated for both non-steatotic and steatotic cells. IC_{50} could be calculated for all drugs except for terbinafine and carbamazepine because these drugs did not induce cytotoxicity in the range of concentrations that could be tested owing to their solubility in the culture medium (Table 3). The lack of carbamazepine and terbinafine cytotoxicity in HepaRG cells was somehow surprising because both drugs induced mitochondrial dysfunction for relatively low concentrations (<100 μM) in isolated mouse liver mitochondria (Porceddu et al., 2012). For amiodarone, atorvastatin, imipramine, lovastatin and perhexiline, IC_{50} and IC_{10} values were similar between non-steatotic and steatotic HepaRG cells (Table 3). For troglitazone, the IC_{50} and IC_{10} were moderately but significantly lower in steatotic cells (Table 3), thus indicating higher cytotoxicity in the context of lipid accumulation. The converse profile was observed with ritonavir with lower cytotoxicity in steatotic HepaRG cells (Table 3).

Selection of drug concentrations to study mtDNA homeostasis

For drugs with calculated IC_{10}, the selected concentrations were close to the IC_{10} and $IC_{10}/5$ in order to perform investigations in condition of slight cytotoxicity or no cytotoxicity, respectively. An exception was for atorvastatin in order to use the same concentration than lovastatin, which belongs to the same pharmacological class. For carbamazepine and terbinafine, for which no IC_{10} could be determined, arbitrary concentrations were chosen. Hence, the working concentrations of the different drugs were as follows: 4 and 20 μM for amiodarone, 1 and 5 μM for atorvastatin and lovastatin, 10 and 300 μM for carbamazepine, 12 and 60 μM for imipramine, 6 and 30 μM for perhexiline, 9 and 45 μM for ritonavir, 10 and 100 μM for terbinafine and 10 and 50 μM for troglitazone. Importantly, the highest working concentrations corresponded to about 6, 8, 24, 25, 47, 83, 100, 107 and 500 x C_{max} for ritonavir, troglitazone, amiodarone, terbinafine, carbamazepine, atorvastatin, imipramine, perhexiline and lovastatin, respectively (Table 3). Thus, for all drugs except lovastatin, these concentrations were lower, equivalent or slightly above than the 100 x C_{max} cutoff classically used for safety assessment in pharmaceutical industry (Porceddu et al., 2012; Dykens et al., 2008). Lovastatin was kept in our study in order to compare its mitochondrial effects with atorvastatin, which belong to the same pharmacological class.

Effects of the 9 drugs on mtDNA levels and expression of ND1 and COX2 at the mRNA and protein levels

In a next series of investigations, we determined the effects of the 9 drugs on mtDNA homeostasis in non-steatotic and steatotic HepaRG cells. For this purpose, HepaRG cells were treated with each drug for 2 weeks to determine their respective effects on mtDNA levels and on the mRNA and protein expression of ND1 and COX2.

None of these drugs decreased mtDNA levels (Figs. 3A, 4A and 5). Instead, mtDNA levels were significantly increased with amiodarone, carbamazepine, imipramine, terbinafine and troglitazone especially for their highest concentrations (Figs. 3A and 5). For amiodarone, carbamazepine and troglitazone, increased mtDNA levels were particularly observed in the absence of steatosis (Fig. 5). The mRNA expression of MT-ND1 and MT-CO2 was also enhanced by different drugs excepted for imipramine, carbamazepine and terbinafine (Figs. 3B and 4B; Table 4). Overall, there was no clear

relationship between mtDNA levels and the mRNA expression of MT-ND1 and MT-CO2 (Figs. 3, 4 and 5; Table 4). Six drugs also significantly increased the mRNA expression of COX4I1 (Table 4).

Next, the protein expression of ND1 and COX2 was investigated. The highest concentrations of imipramine and ritonavir reduced ND1 and COX2 protein levels (Figs. 3C and 4C), whereas the other drugs did not alter the expression of these mtDNA-encoded proteins (data not shown). Ritonavir-induced reduction of ND1 and COX2 protein expression was apparently more pronounced in non-steatotic HepaRG cells as compared to steatotic cells (Fig 4C). Importantly, imipramine and ritonavir did not reduce COX4 protein levels (Figs. 3C and 4C). This result, together with the above-mentioned data, strongly suggested that imipramine and ritonavir impaired mtDNA translation without affecting mtDNA replication and transcription.

Non-steatotic and steatotic HepaRG cells (2 independent cultures) were also treated for 3 days with imipramine (12 and 60 μM) or ritonavir (9 and 45 μM). Imipramine did not reduce ND1 and COX2 protein levels. In contrast, the highest concentration of ritonavir induced about 50% reduction of ND1 protein expression in non-steatotic HepaRG cells, whereas ND1 levels were unchanged in steatotic cells (data not shown). COX2 and COX4 protein levels were not affected by 45 μM ritonavir in non-steatotic and steatotic cells. Taken together, our results suggest that ritonavir-induced impairment of mtDNA translation might occur earlier than with LNZ and imipramine.

Further investigations were also carried out in non-steatotic and steatotic PHH treated or not for 12 days with ritonavir (45 μM) or imipramine (60 μM). Four lots of PHH from different donors were used for these investigations. Our results indicated that ritonavir and imipramine reduced ND1 and COX2 expression in 3 different donors, although the effects were variable between these individuals (Fig. 6). However, these drugs presented no effect in another donor (data not shown). Ritonavir-induced reduction of ND1 expression was more marked in non-steatotic PHH as compared to steatotic PHH (Fig. 6). Interestingly, this effect was also observed in HepaRG cells after 3 days (data not shown) and 2 weeks of ritonavir treatment (Fig. 4).

Effects of imipramine and ritonavir on the expression of MRPL11 and MRPL28

Recent data indicated that some toxicants inducing a mitochondrial stress could impair mitochondrial translation by reducing the levels of different mitochondrial ribosomal proteins including MRPL11 and MRPL28 (Quiros et al., 2017). Hence, we determined whether imipramine and ritonavir could reduce the levels of these proteins. However, MRPL11 and MRPL28 protein levels were not decreased with both drugs after 2 weeks of treatment (data not shown). No change was also observed with 20 μM LNZ (data not shown).

Effects of imipramine and ritonavir on complex I levels and activity, CS activity, mitochondrial respiration and fatty acid oxidation

In order to determine whether imipramine and ritonavir-induced reduction of mtDNA-encoded protein levels could have functional consequences, complex I levels and activity were first measured at the end of the treatments. With imipramine (60 μM), complex I levels and activity were particularly decreased in steatotic cells (Fig. 3D, E), whereas ritonavir (45 μM) induced a stronger reduction of these parameters in non-steatotic cells (Fig. 4D, E). When data collected with both imipramine and ritonavir were taken into account, a robust correlation (R^2=0.89; P<0.001) was observed between complex I levels and complex I activity. Furthermore, a significant correlation existed between ND1 protein expression on the one hand and complex I levels (R^2=0.58; P=0.01), or complex I activity (R^2=0.69; P<0.01), on the other hand. CS activity was also significantly decreased by imipramine (Fig. 3F) and ritonavir (Fig. 4F), in both non-steatotic and steatotic cells.

Oxygen consumption was next assessed in adherent HepaRG cells. Imipramine (60 μM) did not modify mitochondrial respiration (Fig. 3G) but ritonavir (45 μM) significantly reduced the maximal (i.e. FCCP-stimulated) respiration in non-steatotic cells (Fig. 4G). Mitochondrial β-oxidation of palmitic acid was also specifically assessed in adherent HepaRG cells. Imipramine significantly reduced mitochondrial FAO, but only in steatotic HepaRG cells (Fig. 3H). Surprisingly, ritonavir induced a significant increase in mitochondrial FAO, although this effect was observed only in non-steatotic HepaRG cells (Fig. 4H). This effect in non-steatotic cells was accompanied with a significantly higher mRNA expression of peroxisome proliferator-activated receptor-α (PPARα) and its target gene liver carnitine palmitoyltransferase 1

(CPT1A), whereas the expression of medium chain acyl-CoA dehydrogenase (ACADM) and peroxisomal acyl-coenzyme A oxidase (ACOX) was unchanged (data not shown). Finally, it was noteworthy that basal mitochondrial FAO was higher in steatotic cells compared with non-steatotic cells (Figs. 3H and 4H). This is consistent with several reports showing increased mitochondrial FAO in experimental and clinical NAFLD (Begriche et al., 2013; Sunny et al., 2016).

Effects of the 9 drugs on the mRNA expression of key factors involved in mitochondrial biogenesis

In this study, several drugs (i.e. amiodarone, carbamazepine, imipramine, terbinafine, troglitazone) significantly enhanced mtDNA levels (Figs. 3A and 5). Thus, we next determined for all drugs the mRNA expression of four factors playing a key role in mitochondrial biogenesis, namely peroxisome proliferator-activated receptor-γ coactivator 1α and 1β (PGC-1α and PGC-1β), nuclear respiratory factor 1 (NRF1) and mitochondrial transcription factor A (TFAM) (Scarpulla et al., 2012; Villena, 2015; Ploumi et al., 2017). However, different profiles of expression of PGC1A, PGC1B, NRF1 and TFAM were observed among the drugs (Table 4) and there was no apparent relationship between these profiles and the ability of some of these drugs to increase mtDNA levels. An interesting observation was that basal PGC1B expression was significantly reduced by about 25% in steatotic HepaRG cells when compared to non-steatotic HepaRG cells ($P<0.01$) (data not shown). Finally, the expression of POLG and POLRMT was determined since these polymerases play a key role in mitochondrial biogenesis and function (Scarpulla et al., 2012; Vega et al., 2015). Only ritonavir, atorvastatin and lovastatin significantly increased the expression of both POLG and POLRMT, whereas carbamazepine and terbinafine reduced their expression (Table 4). No significant change was observed with the other drugs (Table 4).

Effects of the 9 drugs on AMPK activation

AMPK is another key factor in mitochondrial biogenesis and function, in particular by activating PGC1α (Scarpulla et al., 2012; Vega et al., 2015; Ploumi et al., 2017). Thus, we determined whether the different drugs could activate AMPK by assessing the expression of phospho-AMPKα. Activation of phospho-AMPKα was first validated after a 14-day treatment with A-769662 (Fig. 7A, B). Five drugs, namely

amiodarone, imipramine, lovastatin, terbinafine and troglitazone significantly increased phospho-AMPKα levels after a 14-day treatment at their highest concentrations (Fig. 7A, B). However, for these drugs and A-769662, phospho-AMPKα levels were not reduced in steatotic cells compared to the non-steatotic cells (Fig. 7A, B). Surprisingly, carbamazepine significantly reduced phospho-AMPKα levels compared with the untreated cells (Fig. 7A, B). Finally, we determined whether the expression of phospho-AMPKα levels observed in all conditions of treatment correlated with the corresponding mRNA expression of PGC1α. This correlation tended to be significant (P=0.09) when phospho-AMPKα levels were taken into account but was highly significant (R^2=0.52; P<0.001) when the phospho-AMPKα/total AMPK ratio was considered. In contrast, there was no correlation between phospho-AMPKα levels (or the phospho-AMPKα/total AMPK ratio) with mtDNA levels.

The moderate but significant increased phospho-AMPKα levels observed with 100 μM terbinafine in steatotic cells was surprising since ATP levels were not reduced in this experimental condition (Table 3). Because oxidative stress can also activate AMPK (Horie et al., 2007; Morales-Alamo and Calbet, 2016), we determined whether terbinafine increased the expression of several oxidative stress-related genes, namely nuclear factor erythroid 2-like 2 (NFE2L2, sometimes referred to as Nrf2), heme oxygenase 1 (HMOX1), NAD(P)H quinone dehydrogenase 1 (NQO1), superoxide dismutase 2 (SOD2) and tribbles pseudokinase 3 (TRIB3). However, only HMOX1 and NQO1 expression was significantly increased by 100 μM terbinafine, in particular in non-steatotic cells (data not shown). Hence, energy shortage and oxidative stress were most probably not responsible for AMPKα activation in steatotic HepaRG cells treated with 100 μM terbinafine.

Discussion

Drug-induced alteration of mtDNA homeostasis has been described only with a few drugs, especially with the antiretrovirals NRTIs and some antibiotics (Cohen, 2010; Schon and Fromenty, 2016). In this study, the respective inhibitory effects of ddC (20 μM) and LNZ (20 μM) on mtDNA replication and translation were observed in HepaRG cells after 2 weeks (Fig. 1) but not after 3 days (data not shown). This underlines the importance of an adequate duration of cell treatment in order to detect any significant drug-induced alterations of mtDNA homeostasis and their functional consequences. Such delayed appearance of mitochondrial dysfunction is due to the existence of several threshold effects at different mitochondrial levels (Rossignol et al., 1999; Rossignol et al., 2003). In patients, mitochondrial toxicity and liver injury induced by NRTIs and LNZ usually occurs after several weeks or months of treatment (Spengler et al., 2002; Walker et al., 2004; De Vriese et al., 2006; De Bus et al., 2010). The maximal plasma concentrations (C_{max}) of ddC in patients can be up to 1 μM (Massarella et al., 1996). Thus, the concentration of ddC able to inhibit mtDNA replication in our cellular model represents 20 x C_{max}. Regarding LNZ, (serum) C_{max} in patients can be up to 40 μM (MacGowan, 2003), thus suggesting that the safety margin of this antibiotic is rather low.

Our data strongly suggest that the antidepressant drug imipramine and the antiretroviral protease inhibitor (PI) ritonavir specifically impede mitochondrial translation. Indeed, reduced ND1 and COX2 protein levels induced by imipramine (60 μM) and ritonavir (45 μM) were neither associated with lower expression of the corresponding mtDNA-encoded transcripts, nor with mtDNA depletion (Figs. 3 and 4). Moreover, reduced ND1 and COX2 protein levels were not accompanied by lower protein expression of COX4 (Figs. 3 and 4), MRPL11 and MRPL28 (data not shown), which are nDNA-encoded mitochondrial proteins. Actually, these results were unexpected because mtDNA translation is usually impaired by antibiotics (Cohen, 2010; Schon and Fromenty, 2016). Further investigations will be required to determine whether imipramine and ritonavir could interact with the mitochondrial ribosomes, as shown for the antibiotics chloramphenicol, LNZ and tetracycline (De Vriese et al., 2006; Cohen, 2010; Moullan et al., 2015).

Imipramine and ritonavir also reduced ND1 and COX2 protein expression in PHH from 3 different donors, although the effects were variable among these individuals (Figure 6). This suggests the existence of an inter-individual variability regarding imipramine and ritonavir-induced impairment of mitochondrial translation. Interestingly, genetic susceptibility was reported for antibiotic-induced alterations of mitochondrial protein synthesis and related adverse effects (Hobbie et al., 2008; Garrabou et al., 2017).

Originally developed as an antiretroviral PI, ritonavir is nowadays exclusively used in HIV-positive patients as a pharmacological booster of other PIs. Indeed, by strongly inhibiting CYP3A4, ritonavir increases the bioavailability and plasma concentrations of other PIs (Hull and Montaner, 2011). However, although ritonavir is a CYP3A4 inhibitor, the bioactivation of ritonavir into several metabolites is dependent of this CYP in rodent and human (Kumar et al., 1996; Li et al., 2011). In the mouse, 26 different metabolites have been detected after ritonavir administration (Kumar et al., 1996), thus underlining the complexity of ritonavir metabolism. In this study, ritonavir-induced cytotoxicity (IC_{50}) (Table 1) and impairment of complex I levels and activity (Fig. 4D, E) were significantly lower in steatotic HepaRG cells. Notably, although basal CYP3A4 activity was significantly reduced in untreated steatotic HepaRG cells (Fig. 2), the remaining CYP3A4 activity in cells treated for 2 weeks with 45 μM ritonavir was extremely low (maximum 8%) and equivalent between non-steatotic and steatotic cells (data not shown). Hence, CYP3A4 was probably not responsible for the lower ritonavir toxicity associated with steatosis. Further investigations would be needed to determine why ritonavir is less toxic in steatotic HepaRG cells.

Contrary to ritonavir, the antidiabetic drug troglitazone induced significantly higher cytotoxicity in steatotic HepaRG cells (Table 3). Moreover, the troglitazone-induced adaptive increase in mtDNA levels observed in non-steatotic HepaRG cells was absent in steatotic cells. Importantly, troglitazone can be toxic by itself, in particular by directly impairing mitochondrial function (Nadanaciva et al., 2007; Porceddu et al., 2012). Although troglitazone can be biotransformed into several reactive metabolites, especially via CYP3A4, different investigations suggested that these metabolites are overall less toxic than troglitazone itself (Masubuchi, 2006; Yokoi, 2010; Hosomi et al., 2011). Hence, our data suggest that higher troglitazone cytotoxicity in steatotic HepaRG cells could be due to lower troglitazone biotransformation, including via the CYP3A4 pathway. Troglitazone, the first marketed thiazolidinedione, was actually withdrawn from the market in 2000 because of the occurrence of numerous cases of severe liver failure in patients with type 2

diabetes (Isley, 2003; Labbe et al., 2008; Massart et al., 2017). Because type 2 diabetes most often occurs in obese individuals, troglitazone-induced severe hepatotoxicity might have been favored by preexistent fatty liver in these patients. Interestingly, several experimental investigations showed that rosiglitazone, a thiazolidinedione that is still marketed, was more hepatotoxic in obese mice (Garcia-Ruiz et al., 2007; Massart et al., 2017).

Another important observation in our study was that several of the investigated drugs increased mtDNA levels in HepaRG cells after a treatment of 2 weeks. However, mtDNA levels in treated cells were in general higher in non-steatotic compared to steatotic cells. This pattern was particularly striking with amiodarone, carbamazepine and troglitazone (Fig. 5). Because differences in mtDNA levels could have been explained by changes in mitochondrial biogenesis, we determined the mRNA expression of several factors playing a key role in this process including PGC1A, PGC1B, NRF1, TFAM and phospho-AMPKα. Moreover, POLG expression was also assessed. However, our data could not explain why some drugs increased mtDNA levels in HepaRG cells and why steatosis was associated with lesser mtDNA levels in HepaRG cells treated with amiodarone, carbamazepine and troglitazone. Further investigations will be needed in order to determine whether these effects could be secondary to changes in the activity of these factors, rather than lower mRNA expression. Alternatively, other key factors involved in mtDNA homeostasis might have played a role.

Among the different drugs, only ritonavir (45 μM) significantly increased the mRNA expression of all mitochondrial-related genes investigated in this study, in both non-steatotic and steatotic HepaRG cells (Table 4). Moreover, this drug also enhanced PPARα and CPT1A mRNA expression (data not shown) and palmitate oxidation in non-steatotic cells (Fig. 4G). In contrast, mtDNA levels were unchanged and CS activity was reduced by the treatment, thus suggesting that ritonavir-induced mitochondrial adaptive response was incomplete. Whether the lack of AMPKα activation (Fig. 7) might have played a role in such incomplete response will require further investigations. Notably, CS activity is frequently used as a bona fide marker of mitochondrial content in different pathophysiological situations such as inherited mitochondrial diseases (Guillery et al., 2008) and exercise training (Bishop et al., 2014). Hence, lower CS activity could reflect reduced mitochondrial content in ritonavir-treated cells despite higher mRNA

expression of different nDNA and mtDNA-encoded mitochondrial proteins. Alternatively, ritonavir might directly inhibit the activity of this mitochondrial enzyme.

Previous investigations in HepG2 cells reported that drug-induced cytotoxicity could be different when these cells were cultured in the presence of glucose or galactose, which was reported to favor mitochondrial metabolism (Marroquin et al., 2007; Paech et al., 2017). In the present study, we showed that HepaRG cells cultured for 14 days with glucose or galactose presented similar mitochondrial respiration (Table 2), thus indicating that galactose was not able to augment mitochondrial metabolism in HepaRG cells. Importantly, recent investigations reported that mitochondrial function (e.g. respiration and complex II and IV activities) in differentiated HepaRG cells was close to PHH and significantly superior compared to HepG2 cells (Peyta et al., 2016; Porceddu et al., 2018). Taken together, these data indicate that HepaRG cells present fully functional mitochondria and that their culture with galactose is not able to further enhance mitochondrial capacity.

Because drug-induced alteration of mtDNA translation might have been overlooked in the past, especially for drugs that are not antibiotics, we would recommend to include studies on mtDNA translation to investigators wishing to better understand how some compounds can alter mitochondrial function. To do so, the HepaRG cell line is a suitable model because drug toxicity can be studied over 2 weeks (present study) or longer (Anthérieu et al., 2012). Moreover, this cell line could be appropriate to study drug-induced modulation of mitochondrial biogenesis. Indeed, the expression of several major mitochondrial biogenesis factors (e.g. PGC-1α, PGC-1β, phospho-AMPKα) was significantly increased, or decreased, by several investigated drugs. Interestingly, there was a significant correlation between the PGC1α mRNA expression and the phospho-AMPKα/total AMPK ratio in treated HepaRG cells. Despite these advantages, HepaRG cells present some limitations, as previously pointed out (Bucher et al., 2016; Michaut et al., 2016). For instance, this cell line derives from one female patient and thus does not allow to disclose gender differences or genetic susceptibility. Supplementary investigations in PHH can help to tackle these issues.

Acknowledgments:

We are grateful to the Institut National de la Santé et de la Recherche Médicale (INSERM) for its constant support.

Conflict of interest:

Bernard Fromenty reports personal fees from Alfasigma France and Novo Nordisk, outside the submitted work.

Authorship Contributions:

Participated in research design: *Labbe and Fromenty*.

Conducted experiments: *Le Guillou and Bucher*.

Provided analytical reagents: *Lombès.*

Performed data analysis: *Le Guillou, Bucher, Begriche and Hoët.*

Wrote or contributed to the writing of the manuscript*: Le Guillou, Begriche, Lombès and Fromenty*.

References

Agier V, Oliviero P, Lainé J, L'Hermitte-Stead C, Girard S, Fillaut S, Jardel C, Bouillaud F, Bulteau AL, and Lombès A (2012) Defective mitochondrial fusion, altered respiratory function, and distorted cristae structure in skin fibroblasts with heterozygous OPA1 mutations. *Biochim Biophys Acta* **1822**:1570–1580.

Anthérieu S, Chesné C, Li R, Guguen-Guillouzo C, and Guillouzo A (2012) Optimization of the HepaRG cell model for drug metabolism and toxicity studies. *Toxicol In Vitro* **26**:1278–1285.

Anthérieu S, Rogue A, Fromenty B, Guillouzo A, and Robin M-A (2011) Induction of vesicular steatosis by amiodarone and tetracycline is associated with up-regulation of lipogenic genes in HepaRG cells. *Hepatology* **53**:1895–1905.

Aubert J, Begriche K, Knockaert L, Robin MA, and Fromenty B (2011) Increased expression of cytochrome P450 2E1 in nonalcoholic fatty liver disease: Mechanisms and pathophysiological role. *Clin Res Hepatol Gastroenterol* **35**:630–637.

Begriche K, Igoudjil A, Pessayre D, and Fromenty B (2006) Mitochondrial dysfunction in NASH: causes, consequences and possible means to prevent it. *Mitochondrion* **6**:1–28.

Begriche K, Massart J, Robin M-A, Bonnet F, and Fromenty B (2013) Mitochondrial adaptations and dysfunctions in nonalcoholic fatty liver disease. *Hepatology* **58**:1497–1507.

Begriche K, Massart J, Robin M-A, Borgne-Sanchez A, and Fromenty B (2011) Drug-induced toxicity on mitochondria and lipid metabolism: mechanistic diversity and deleterious consequences for the liver. *J Hepatol* **54**:773–794.

Bishop DJ, Granata C, and Eynon N (2014) Can we optimise the exercise training prescription to maximise improvements in mitochondria function and content? *Biochim Biophys Acta* **1840**:1266–1275.

Bucher S, Jalili P, Le Guillou D, Begriche K, Rondel K, Martinais S, Zalko D, Corlu A, Robin MA, and Fromenty B (2017) Bisphenol A induces steatosis in HepaRG cells using a model of perinatal exposure. *Environ Toxicol* **32**:1024–1036.

Cohen BH (2010) Pharmacologic effects on mitochondrial function. *Dev Disabil Res Rev* **16**:189–199.

De Bus L, Depuydt P, Libbrecht L, Vandekerckhove L, Nollet J, Benoit D, Vogelaers D, and Van Vlierberghe H (2010) Severe drug-induced liver injury associated with prolonged use of linezolid. *J Med Toxicol* **6**:322–326.

De Vriese AS, Coster RV, Smet J, Seneca S, Lovering A, Van Haute LL, Vanopdenbosch LJ, Martin J-J, Groote CC, Vandecasteele S, and Boelaert JR (2006) Linezolid-induced inhibition of mitochondrial protein synthesis. *Clin Infect Dis* **42**:1111–1117.

Deschamps D, DeBeco V, Fisch C, Fromenty B, Guillouzo A, and Pessayre D (1994) Inhibition by perhexiline of oxidative phosphorylation and the beta-oxidation of fatty acids: possible role in pseudoalcoholic liver lesions. *Hepatology* **19**:948–961.

Dykens JA, Jamieson JD, Marroquin LD, Nadanaciva S, Xu JJ, Dunn MC, Smith AR, and Will Y (2008) In vitro assessment of mitochondrial dysfunction and cytotoxicity of nefazodone, Trazodone, and Buspirone. *Toxicol Sci* **103**:335–345.

Eakins J, Bauch C, Woodhouse H, Park B, Bevan S, Dilworth C, and Walker P (2016) A combined in vitro approach to improve the prediction of mitochondrial toxicants. *Toxicol In Vitro* **34**:161–170.

Fromenty B (2013) Drug-induced liver injury in obesity. *J Hepatol* **58**:824–826.

Fromenty B, Fisch C, Berson A, Letteron P, Larrey D, and Pessayre D (1990) Dual effect of amiodarone on mitochondrial respiration. Initial protonophoric uncoupling effect followed by inhibition of the respiratory chain at the levels of complex I and complex II. *J Pharmacol Exp Ther* **255**:1377–1384.

García-Ruiz I, Rodríguez-Juan C, Díaz-Sanjuán T, Martínez MA, Muñoz-Yagüe T, and Solís-Herruzo JA (2007) Effects of rosiglitazone on the liver histology and mitochondrial function in ob/ob mice. *Hepatology* **46**:414–423.

Garrabou G, Soriano À, Pinós T, Casanova-Mollà J, Pacheu-Grau D, Morén C, García-Arumí E, Morales M, Ruiz-Pesini E, Catalán-Garcia M, Milisenda JC, Lozano E, Andreu AL, Montoya J, Mensa J, and Cardellach F (2017) Influence of mitochondrial genetics on the mitochondrial toxicity of linezolid in blood cells and skin nerve fibers. *Antimicrob Agents Chemother* **61**:e00542–17.

Guillery O, Malka F, Frachon P, Milea D, Rojo M, and Lombès A (2008) Modulation of mitochondrial morphology by bioenergetics defects in primary human fibroblasts. *Neuromuscul Disord* **18**:319–330.

Hobbie SN, Akshay S, Kalapala SK, Bruell CM, Shcherbakov D, and Böttger EC (2008) Genetic analysis of interactions with eukaryotic rRNA identify the mitoribosome as target in aminoglycoside ototoxicity. *Proc Natl Acad Sci USA* **105**:20888–20893.

Horie T, Ono K, Nagao K, Nishi H, Kinoshita M, Kawamura T, Wada H, Shimatsu A, Kita T, and Hasegawa K (2008) Oxidative stress induces GLUT4 translocation by activation of PI3-K/Akt and dual AMPK kinase in cardiac myocytes. *J Cell Physiol* **215**:733–742.

Hosomi H, Fukami T, Iwamura A, Nakajima M, and Yokoi T (2011) Development of a highly sensitive cytotoxicity assay system for CYP3A4-mediated metabolic activation. *Drug Metab Dispos* **39**:1388–1395.

Hull MW, and Montaner JSG (2011) Ritonavir-boosted protease inhibitors in HIV therapy. *Ann Med* **43**:375–388.

Isley WL (2003) Hepatotoxicity of thiazolidinediones. *Expert Opin Drug Saf* **2**:581–586.

Kamalian L, Chadwick AE, Bayliss M, French NS, Monshouwer M, Snoeys J, and Park BK (2015) The utility of HepG2 cells to identify direct mitochondrial dysfunction in the absence of cell death. *Toxicol In Vitro* **29**:732–740.

Kumar GN, Rodrigues AD, Buko AM, and Denissen JF (1996) Cytochrome P450-mediated metabolism of the HIV-1 protease inhibitor ritonavir (ABT-538) in human liver microsomes. *J Pharmacol Exp Ther* **277**:423–431.

Labbe G, Pessayre D, and Fromenty B (2008) Drug-induced liver injury through mitochondrial dysfunction: mechanisms and detection during preclinical safety studies. *Fundam Clin Pharmacol* **22**:335–353.

Li F, Lu J, and Ma X (2011) Metabolomic screening and identification of the bioactivation pathways of ritonavir. *Chem Res Toxicol* **24**:2109–2114.

MacGowan AP (2003) Pharmacokinetic and pharmacodynamic profile of linezolid in healthy volunteers and patients with Gram-positive infections. *J Antimicrob Chemother* **51**:ii17–ii25.

Marroquin LD, Hynes J, Dykens JA, Jamieson JD, and Will Y (2007) Circumventing the Crabtree effect: replacing media glucose with galactose increases susceptibility of HepG2 cells to mitochondrial toxicants. *Toxicol Sci* **97**:539–547.

Marroquin L, Swiss R, and Will Y (2014) Identifying compounds that induce opening of the mitochondrial permeability transition pore in isolated rat liver mitochondria. *Curr Protoc Toxicol* **60**:25.4.1-17.

Massarella JW, Nazareno LA, Passe S, and Min B (1996) The effect of probenecid on the pharmacokinetics of zalcitabine in HIV-positive patients. *Pharm Res* **13**:449–452.

Massart J, Begriche K, Moreau C, and Fromenty B (2017) Role of nonalcoholic fatty liver disease as risk factor for drug-induced hepatotoxicity. *J Clin Transl Res* **3**:212–232.

Masubuchi Y (2006) Metabolic and non-metabolic factors determining troglitazone hepatotoxicity: a review. *Drug Metab Pharmacokinet* **21**:347–356.

Michaut A, Le Guillou D, Moreau C, Bucher S, McGill MR, Martinais S, Gicquel T, Morel I, Robin M-A, Jaeschke H, and Fromenty B (2016) A cellular model to study drug-induced liver

injury in nonalcoholic fatty liver disease: Application to acetaminophen. *Toxicol Appl Pharmacol* **292**:40–55.

Michaut A, Moreau C, Robin M-A, and Fromenty B (2014) Acetaminophen-induced liver injury in obesity and nonalcoholic fatty liver disease. *Liver Int* **34**:e171-179.

Morales-Alamo D, and Calbet JAL (2016) AMPK signaling in skeletal muscle during exercise: Role of reactive oxygen and nitrogen species. *Free Radic Biol Med* **98**:68–77.

Moullan N, Mouchiroud L, Wang X, Ryu D, Williams EG, Mottis A, Jovaisaite V, Frochaux MV, Quiros PM, Deplancke B, Houtkooper RH, and Auwerx J (2015) Tetracyclines disturb mitochondrial function across eukaryotic models: A call for caution in biomedical research. *Cell Rep* **10**:1681–1691.

Nadanaciva S, Dykens JA, Bernal A, Capaldi RA, and Will Y (2007) Mitochondrial impairment by PPAR agonists and statins identified via immunocaptured OXPHOS complex activities and respiration. *Toxicol Appl Pharmacol* **223**:277–287.

Paech F, Bouitbir J, and Krähenbühl S (2017) Hepatocellular toxicity associated with tyrosine kinase inhibitors: mitochondrial damage and inhibition of glycolysis. *Front Pharmacol* **8**:367.

Peyta L, Jarnouen K, Pinault M, Guimaraes C, Pais de Barros JP, Chevalier S, Dumas JF, Maillot F, Hatch GM, Loyer P, and Servais S (2016) Reduced cardiolipin content decreases respiratory chain capacities and increases ATP synthesis yield in the human HepaRG cells. *Biochim Biophys Acta* **1857**:443–53.

Ploumi C, Daskalaki I, and Tavernarakis N (2017) Mitochondrial biogenesis and clearance: a balancing act. *FEBS J* **284**:183–195.

Porceddu M, Buron N, Roussel C, Labbe G, Fromenty B, and Borgne-Sanchez A (2012) Prediction of liver injury induced by chemicals in human with a multiparametric assay on isolated mouse liver mitochondria. *Toxicol Sci* **129**:332–345.

Porceddu M, Buron N, Rustin P, Fromenty B, and Borgne-Sanchez A (2018) In vitro Assessment of Mitochondrial Toxicity to Predict Drug-Induced Liver Injury, in *Drug-Induced Liver Toxicity*, pp 283–300, Chen M, Will Y, eds. Springer, Berlin, Germany.

Quirós PM, Prado MA, Zamboni N, D'Amico D, Williams RW, Finley D, Gygi SP, and Auwerx J (2017) Multi-omics analysis identifies ATF4 as a key regulator of the mitochondrial stress response in mammals. *J Cell Biol* **216**:2027–2045.

Rossignol R, Faustin B, Rocher C, Malgat M, Mazat J-P, and Letellier T (2003) Mitochondrial threshold effects. *Biochem J* **370**:751–762.

Rossignol R, Malgat M, Mazat J-P, and Letellier T (1999) Threshold effect and tissue specificity implication for mitochondrial cytopathies. *J Biol Chem* **274**:33426–33432.

Scarpulla RC, Vega RB, and Kelly DP (2012) Transcriptional integration of mitochondrial biogenesis. *Trends Endocrinol Metab* **23**:459–466.

Schon EA, and Fromenty B (2015) Mitochondria in Liver Disease, in *Mitochondria in Liver Disease* pp 283–314, Kaplowitz N, Han D, eds. Taylor & Francis, New-York.

Spengler U, Lichterfeld M, and Rockstroh JK (2002) Antiretroviral drug toxicity – a challenge for the hepatologist? *J Hepatol* **36**:283–294.

Sunny NE, Bril F, and Cusi K (2017) Mitochondrial Adaptation in Nonalcoholic Fatty Liver Disease: Novel Mechanisms and Treatment Strategies. *Trends Endocrinol Metab* **28**:250–260.

Vega RB, Horton JL, and Kelly DP (2015) Maintaining ancient organelles: mitochondrial biogenesis and maturation. *Circ Res* **116**:1820–1834.

Villena JA (2015) New insights into PGC-1 coactivators: redefining their role in the regulation of mitochondrial function and beyond. *FEBS J* **282**:647–672.

Walker UA, Bäuerle J, Laguno M, Murillas J, Mauss S, Schmutz G, Setzer B, Miquel R, Gatell JM, and Mallolas J (2004) Depletion of mitochondrial DNA in liver under antiretroviral therapy with didanosine, stavudine, or zalcitabine. *Hepatology* **39**:311–317.

Wallace DC, Fan W, and Procaccio V (2010) Mitochondrial Energetics and Therapeutics. *Annu Rev Pathol Mech Dis* **5**:297–348.

Will Y, and Dykens J (2014) Mitochondrial toxicity assessment in industry--a decade of technology development and insight. *Expert Opin Drug Metab Toxicol* **10**:1061–1067.

Woolsey SJ, Mansell SE, Kim RB, Tirona RG, and Beaton MD (2015) Cytochrome P450 3A Activity and Expression in Non-Alcoholic Fatty Liver Disease. *Drug Metab Dispos* **43**:1484–1490.

Yokoi T (2010) Troglitazone. *Handb Exp Pharmacol* **196**:419–435.

Footnotes:

This work (including Dounia Le Guillou's PhD stipend) has been founded by Sanofi. Simon Bucher was recipient of a fellowship from the Région Bretagne and the Agence Nationale de la Recherche (STEATOX project; "ANR-13-CESA-0009").

Figure Legends:

Fig. 1 Mitochondrial effects of zalcitabine (left) and linezolid (right)

Non-steatotic HepaRG cells were untreated (Ctrl) or treated with 20 μM zalcitabine (ddC) or 20 μM linezolid (LNZ) for 2 weeks and several mitochondrial parameters were measured at the end of the treatment. **A** mtDNA levels. **B** mRNA expression of *MT-ND1*, *MT-CO2* and *COX4I1*. **C** Protein expression of ND1, COX2, COX4 and β-actin. Numbers below the bands indicate the mean of the relative intensities for 3 independent cultures. **D** Complex I levels and activity. Results are means ± SEM for 3 independent cultures (**D**) or 5 independent cultures (**A** and **B**). Statistical analysis was performed with a t-test. *Significantly different from untreated HepaRG cells.

Fig. 2 Main features of the in vitro HepaRG cell model of steatosis induced by lipid overload

To induce steatosis, HepaRG cells were treated for 2 weeks with a mixture of stearic acid (150 μM) and oleic acid (150 μM). Non-steatotic (NS) and steatotic (S) cells were then compared for different parameters linked to steatosis. **A** Lipid accumulation as assessed by levels of cellular triglycerides and neutral lipids (Nile red staining). **B** mRNA expression of *APOA4*, *PLIN1*, *PLIN2*, *CYP2E1* and *CYP3A4*. **C** Activity of CYP2E1 and CYP3A4. Results are means ± SEM for 5 independent cultures. Statistical analysis was performed with a *t*-test. *Significantly different from NS HepaRG cells.

Fig. 3 Mitochondrial effects of imipramine

Non-steatotic (NS) and steatotic (S) HepaRG cells were untreated (Ctrl) or treated with 12 or 60 μM imipramine for 2 weeks and several mitochondrial parameters were measured at the end of the treatment. **A** mtDNA levels. **B** mRNA expression of *MT-ND1* and *MT-CO2*. **C** Protein expression of ND1, COX2, COX4 and β-actin. Numbers below the bands indicate the mean of the relative intensities for 3 independent cultures. **D** Complex I levels. **E** Complex I activity **F** Citrate synthase (CS) activity. **G** Basal and maximal mitochondrial respiration. **H** Palmitate oxidation. Results are means ± SEM for 3 independent cultures (**D**, **E** and **F**), 4 independent cultures (**G**, **G** and **H**) or 6 independent cultures (**A**).

Statistical analysis was performed with a two-way ANOVA: T, effect of treatment, S, effect of steatosis, TxS, interaction between treatment and steatosis. Individual means were then compared with the post hoc Bonferroni test. *Significantly different from untreated NS or S cells. †Significantly different from NS cells (P<0.05).

Fig. 4 Mitochondrial effects of ritonavir

Non-steatotic (NS) and steatotic (S) HepaRG cells were untreated (Ctrl) or treated with 9 or 45 μM ritonavir for 2 weeks and several mitochondrial parameters were measured at the end of the treatment. **A** mtDNA levels. **B** mRNA expression of *MT-ND1* and *MT-CO2*. **C** Protein expression of ND1, COX2, COX4 and β-actin. Numbers below the bands indicate the mean of the relative intensities for 3 independent cultures. **D** Complex I levels. **E** Complex I activity **F** Citrate synthase (CS) activity. **G** Basal and maximal mitochondrial respiration. **H** Palmitate oxidation. Results are means ± SEM for 3 independent cultures (**D**, **E** and **F**), 4 independent cultures (**B**, **G** and **H**) or 6 independent cultures (**A**). Statistical analysis was performed with a two-way ANOVA: T, effect of treatment, S, effect of steatosis, TxS, interaction between treatment and steatosis. Individual means were then compared with the post hoc Bonferroni test. *Significantly different from untreated NS or S cells. †Significantly different from NS cells treated by the same concentration of ritonavir (P<0.05).

Fig. 5 Drug-induced modulation of mtDNA levels

Non-steatotic (NS) and steatotic (S) HepaRG cells were untreated (Ctrl) or treated for 2 weeks with different concentrations of amiodarone, atorvastatin, carbamazepine, lovastatin, perhexiline, terbinafine or troglitazone and mtDNA levels were measured at the end of the treatment. Results are means ± SEM for 6 independent cultures. Statistical analysis was performed with a two-way ANOVA: T, effect of treatment, S, effect of steatosis, TxS, interaction between treatment and steatosis. Individual means were then compared with the post hoc Bonferroni test. *Significantly different from untreated NS or S cells. †Significantly different from NS cells treated by the same concentration of the drug (P<0.05).

Fig. 6 Effect of imipramine and ritonavir on ND1, COX2 and COX4 expression in primary human hepatocytes

Non-steatotic (NS) and steatotic (S) primary human hepatocytes (PHH) from 3 different donors were untreated (Ctrl) or treated with 45 μM ritonavir (RIT) or 60 μM imipramine (IMI) for 12 days and protein expression of ND1, COX2, COX4 was assessed at the end of the treatments. β-Actin was used as loading control.

Fig. 7 Drug-induced AMPK activation

Non-steatotic (NS) and steatotic (S) HepaRG cells were untreated (Ctrl) or treated for 2 weeks with 30 μM A-769662 (A-76), 20 μM amiodarone (AMI), 5 μM atorvastatin (ATO), 300 μM carbamazepine (CAR), 60 μM imipramine (IMI), 5 μM lovastatin (LOV), 30 μM perhexiline (PER), 45 μM ritonavir (RIT), 100 μM terbinafine (TER) or 50 μM troglitazone (TRO) and levels of phospho-AMPKα (P-AMPKα), total AMPKα (AMPKα) and β-actin were assessed at the end of the treatment. **A** Representative western blots for the different groups of treatment. **B** Quantification of phospho-AMPKα levels. Results are means ± SEM for 3 independent cultures. Statistical analysis between untreated cells and cells treated with each drug was performed with a two-way ANOVA: T, effect of treatment. Individual means were then compared with the post hoc Bonferroni test. *Significantly different from untreated NS or S cells ($P<0.05$).

Table 1. List of the primers used in this study

Gene symbol	Gene name	Forward primer	Reverse primer
APOA4	apolipoprotein A4	CAGTGTGGCAAGAAACTCCT	GTAGTCCCACATCACCGTG
ACADM	acyl-CoA dehydrogenase, C-4 to C-12 straight chain	TTTGGGGAGAATGACTGAGG	TGGATCAGAACGTGCCAATA
ACOX1	acyl-CoA oxidase 1	GATGAAGTATGCCCAGGTGAAG	CACAAGGAAGGACCTGACAAA
COX4I1	cytochrome c oxidase subunit 4I1	CAGAATGTTGGCTACCAGGG	GGTCACGCCGATCCATATAAG
CPT1A	carnitine palmitoyltransferase 1A	CGGGAGGAAATCAAACCAATTC	CTGGGATCCGGGAAGTATTAAA
CYP2E1	cytochrome P450 family 2 subfamily E member 1	TTGAAGCCTCTCGTTGACCC	CGTGGTGGGATACAGCAA
CYP3A4	cytochrome P450 family 3 subfamily A member 4	CTTCATCCAATGGACTGCATAAAT	TCCCAAGTATAACACTCTACACAGACAA
GAPDH	glyceraldehyde-3-phosphate dehydrogenase	ATGACATCAAGAAGGTGGTG	CATACCAGGAAATGAGCTTG
HMOX1	heme oxygenase 1	ACTTTCAGAAGGGCCAGGT	TTGTTGCGCTCAATCTCCT
MT-CO2	mitochondrially encoded cytochrome c oxidase subunit II	CTGAACCTACGAGTACACCG	TTAATTCTAGGACGATGGGC
MT-ND1	mitochondrially encoded NADH dehydrogenase subunit 1	CCCTAAAACCCGCCACATCT	GAGCGATGGTGAGAGCTAAGGT
NFE2L2	nuclear factor, erythroid 2 like 2	TCAGCATGCTACGTGATGAAG	TTTGCTGCAGGGAGTATTCA
NQO1	NAD(P)H quinone dehydrogenase 1	ACGTCCTTCAACTATGCCATG	TTACCTGTGATGTCCTTTCTGG
NRF1	nuclear respiratory factor 1	GCCACAGCCACACATAGTATAG	CGTACCAACCTGGATAAGTGAG
PLIN1	perilipin 1	TGGTCCTCATGATCCTCCTC	GTTGTCGATGTCCCGGAATT
PLIN2	perilipin 2	CCATTCTACTGTTCACCTGATTGA	ACCCATGAGAGGTAGAGCTTAT
POLG	DNA polymerase gamma, catalytic subunit	GGCTGTCCAGGAAGAGTTTATG	CCACAAGCATGAGGTGTAAGT
POLRMT	RNA polymerase mitochondrial	GGACTCCAAGGTCAAGCAAATA	TCTTCTGCTTACGTGTGTTGG
PPARA	peroxisome proliferator activated receptor alpha	GTTCTGGAAGCTTTGGCTTTAC	GAAAGCGTGTCCGTGATGA
PPARGC1A (PGC1A)	PPARG coactivator 1 alpha	AGTGGTGCAGTGACCAATCA	CTGCTAGCAAGTTTGCCTCA
PPARGC1B (PGC1B)	PPARG coactivator 1 beta	GTACATTCAAAATCTCTCCAGCGACATG	GAGGGCTCGTTCCTCAGGGCA
SOD2	superoxide dismutase 2	GGGTTGGCTTGGTTTCAATA	CTGATTTGGACAAGCAGCAA
TFAM	transcription factor A, mitochondrial	GCTCAGAACCCAGATGCAAA	TGCCACTCCGCCCTATAA
TRIB3	tribbles pseudokinase 3	CCCTGCTCACAGAGATGACA	GCAGCTGGTTTGTTTGTGAA

Table 2. Effects of glucose and galactose on mitochondrial function in HepaRG cells

		Mito Stress Test profile parameters		
Substrate for culture	Substrate for respiration	Basal respiration	Maximal respiration	ATP production
Glucose	Glucose	3.7 ± 0.2	17.9 ± 1.7	2.8 ± 0.3
Galactose	Glucose	3.7 ± 0.3	17.5 ± 2.0	2.8 ± 0.3
Glucose	Galactose	3.6 ± 0.2	16.8 ± 2.1	2.8 ± 0.2
Galactose	Galactose	3.8 ± 0.2	15.0 ± 1.7	2.9 ± 0.1

HepaRG cells were cultured in a William's E medium with 11.1 mM glucose or without glucose but supplemented with 11.1 mM galactose. After 14 days, mitochondrial respiration was measured for each culture condition (i.e. glucose or galactose) in the presence of L-glutamine/pyruvate/glucose or L-glutamine/pyruvate/galactose with glucose and galactose at the same concentration (10 mM). Three mitochondrial parameters (i.e. respiration rates in nmol/min/10^6 cells) provided by the Mito Stress Test profile are shown. Results are means ± SEM for 3 independent cultures.

Table 3. Drug-induced cytotoxicity in non-steatotic and steatotic HepaRG cells

Drugs	IC_{50} (µM)		IC_{10} (µM)		C_{max} (µM)
	Non-steatotic	Steatotic	Non-steatotic	Steatotic	
Amiodarone	29.8 ± 0.6	34.2 ± 0.6	24.6 ± 0.7	23.4 ± 0.7	0.81
Atorvastatin	19.3 ± 0.5	17.0 ± 0.5	15.0 ± 0.6	11.0 ± 0.6	0.06
Carbamazepine	> 300	> 300	> 300	> 300	6.43
Imipramine	79.8 ± 0.5	75.6 ± 0.5	66.2 ± 0.6	63.0 ± 0.6	0.6
Lovastatin	13.8 ± 0.6	10.8 ± 0.6	6.5 ± 0.7	4.0 ± 0.6	0.01
Perhexiline	32.4 ± 1.8	33.0 ± 0.7	30.7 ± 0.8	30.6 ± 0.6	0.28
Ritonavir	51.3 ± 0.5	58.8 ± 0.6*	43.8 ± 0.6	46.8 ± 0.6	7.07
Terbinafine	> 100	> 100	> 100	> 100	4
Troglitazone	70.4 ± 0.5	58.6 ± 0.6*	66.1 ± 0.5	51.1 ± 0.7*	6.6

Cytotoxicity was assessed by measuring cellular ATP levels and IC_{50} and IC_{10} values were subsequently calculated. Results are means ± SEM for 4 independent cultures. Statistical analysis was performed with a *t*-test. *Significantly different from non-steatotic HepaRG cells (P<0.05). C_{max} values are from Porceddu et al. 2012.

Table 4. Effects of the 9 different drugs on the mRNA expression of different mitochondrial-related genes.

		MT-ND1	*MT-CO2*	*COX4I1*	*PGC1A*	*PGC1B*	*NRF1*	*TFAM*	*POLG*	*POLRMT*
Amiodarone										
20 µM	NS	T 1.30 ± 0.06	1.34 ± 0.30	T 1.15 ± 0.16	T **2.26 ± 0.41***	0.74 ± 0.10	1.09 ± 0.21	1.00 ± 0.12	0.99 ± 0.12	0.95 ± 0.14
	S	1.22 ± 0.05	1.13 ± 0.15	1.41 ± 0.12	**1.98 ± 0.14***	0.63 ± 0.06	1.10 ± 0.02	1.11 ± 0.08	1.13 ± 0.04	1.01 ± 0.07
Atorvastatin										
5 µM	NS	T 1.51 ± 0.25	T **2.16 ± 0.43***	T 1.68 ± 0.31	1.06 ± 0.02	T 1.35 ± 0.10	T **2.95 ± 0.88***	1.52 ± 0.18	T 2.14 ± 0.56	T 1.84 ± 0.40
	S	1.41 ± 0.26	1.57 ± 0.40	1.71 ± 0.23	1.13 ± 0.04	**1.25 ± 0.15***	2.02 ± 0.45	1.45 ± 0.08	1.84 ± 0.27	1.55 ± 0.26
Carbamazepine										
300 µM	NS	1.02 ± 0.07	1.45 ± 0.34	0.94 ± 0.04	T 0.77 ± 0.12	0.84 ± 0.13	0.91 ± 0.11	0.85 ± 0.04	0.87 ± 0.09	T 0.86 ± 0.06
	S	0.85 ± 0.15	1.41 ± 0.19	0.88 ± 0.15	0.63 ± 0.10	0.75 ± 0.21	1.11 ± 0.53	0.83 ± 0.20	0.87 ± 0.11	0.73 ± 0.12
Imipramine										
60 µM	NS	T 1.16 ± 0.04	0.96 ± 0.18	T **1.53 ± 0.11***	T **3.20 ± 0.22***	1.03 ± 0.14	1.04 ± 0.11	1.06 ± 0.01	1.18 ± 0.08	1.12 ± 0.05
	S	1.22 ± 0.12	1.05 ± 0.19	**1.85 ± 0.21***	**3.25 ± 0.33***	0.89 ± 0.10	1.02 ± 0.10	1.08 ± 0.08	1.23 ± 0.14	1.00 ± 0.06
Lovastatin										
5 µM	NS	T **1.23 ± 0.03***	T 1.32 ± 0.22	T **1.27 ± 0.06***	T 1.36 ± 0.14	T, S 1.37 ± 0.14	1.00 ± 0.14	T 1.26 ± 0.11	T 1.37 ± 0.15	T 1.33 ± 0.13
	S	1.15 ± 0.03	1.68 ± 0.11	**1.34 ± 0.05***	1.38 ± 0.09	1.05 ± 0.08	0.97 ± 0.13	1.41 ± 0.08	1.29 ± 0.10	1.20 ± 0.08
Perhexiline										
30 µM	NS	0.92 ± 0.07	T 1.38 ± 0.06	T 1.23 ± 0.04	T **1.89 ± 0.19***	0.93 ± 0.11	0.91 ± 0.05	0.92 ± 0.15	0.91 ± 0.09	T 0.81 ± 0.06
	S	0.87 ± 0.19	1.36 ± 0.20	1.26 ± 0.12	**1.78 ± 0.08***	0.82 ± 0.11	0.92 ± 0.06	0.95 ± 0.05	0.91 ± 0.09	0.84 ± 0.05
Ritonavir										
45 µM	NS	T **1.93 ± 0.17***	T 1.36 ± 0.23	T, S **1.82 ± 0.10***	T **3.47 ± 0.28***	T, S 1.48 ± 0.10	T **1.84 ± 0.18***	T 1.72 ± 0.12	T 1.46 ± 0.13	T 1.40 ± 0.15
	S	**1.72 ± 0.14***	**1.76 ± 0.17***	**2.17 ± 0.08*†**	**2.81± 0.36***	1.12 ± 0.23	**1.85 ± 0.08***	**2.05 ± 0.36***	**1.73 ± 0.23***	1.38 ± 0.18
Terbinafine										
100 µM	NS	T **0.73 ± 0.06***	1.34 ± 0.29	0.95 ± 0.07	1.28 ± 0.15	T **0.56 ± 0.07***	0.89 ± 0.17	T **0.74 ± 0.09***	T 0.75 ± 0.03	T **0.63 ± 0.02***
	S	0.84 ± 0.09	1.48 ± 0.31	1.04 ± 0.14	1.00 ± 0.12	0.67 ± 0.12	1.25 ± 0.35	0.96 ± 0.04	0.97 ± 0.11	0.88 ± 0.09
Troglitazone										
50 µM	NS	T 1.38 ± 0.08	T **2.07 ± 0.26***	1.10 ± 0.01	1.13 ± 0.06	T 1.37 ± 0.17	1.00 ± 0.05	1.07 ± 0.06	1.00 ± 0.08	1.09 ± 0.06
	S	**1.46 ± 0.24***	**2.18 ± 0.26***	1.43 ± 0.24	1.19 ± 0.24	1.23 ± 0.19	0.93 ± 0.06	1.31 ± 0.17	1.39 ± 0.29	1.17 ± 0.08

Results, expressed as a fold-change of untreated non-steatotic (NS) cells, are means ± SEM for 4 independent cultures. Statistical analysis was performed with a two-way ANOVA: T, effect of treatment, S, effect of steatosis. Individual means were then compared with the post hoc Bonferroni test. *Significantly different from untreated NS or S cells. †Significantly different from NS cells ($P<0.05$). Data in grey boxes indicate significant differences with the two-way ANOVA. Data in bold characters indicate significant differences with the post hoc Bonferroni test.

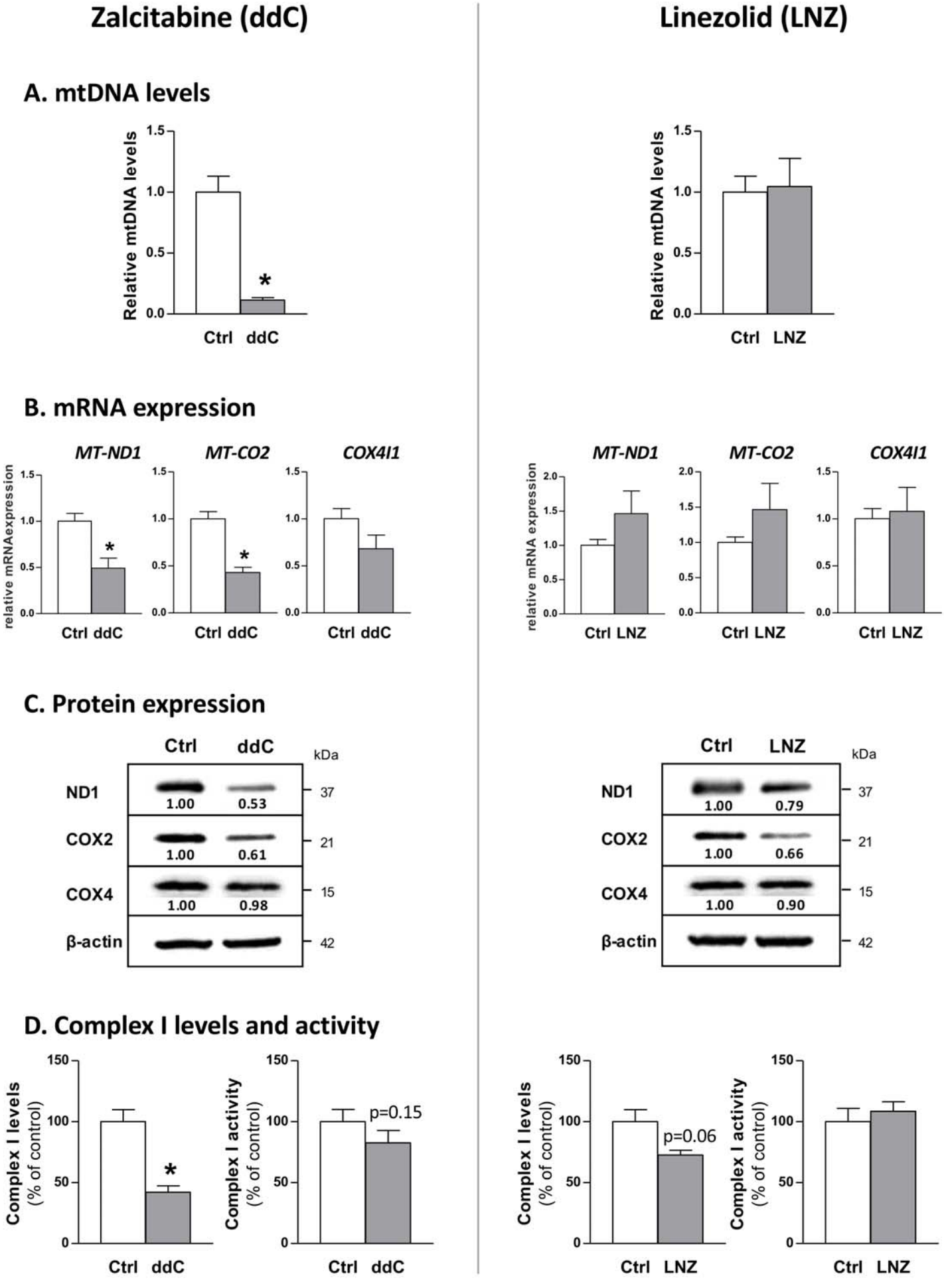

Figure 1: Mitochondrial effects of zalcitabine (left) and linezolid (right)

A. Lipid accumulation

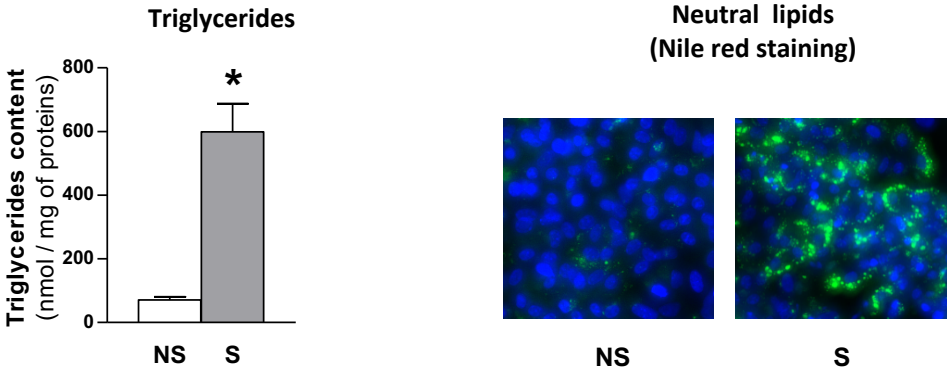

B. mRNA expression

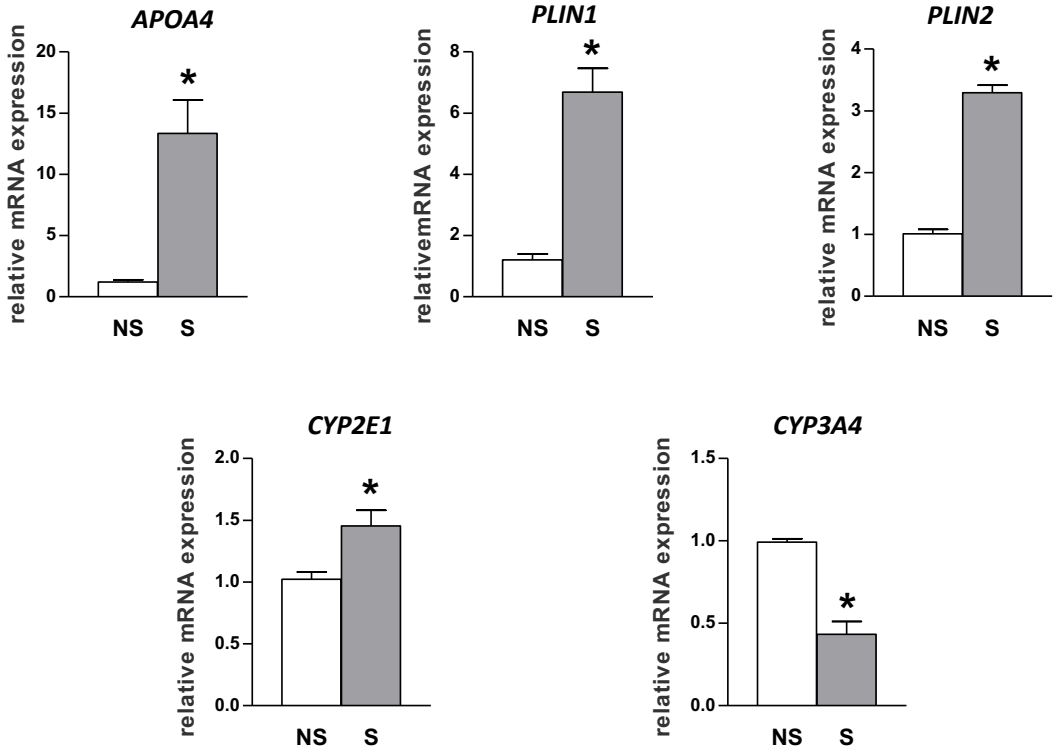

C. CYP activity

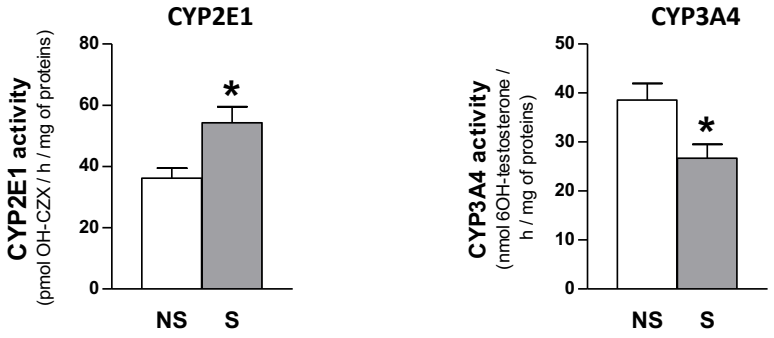

Figure 2: Main features of the in vitro HepaRG cell model of steatosis induced by lipid overload

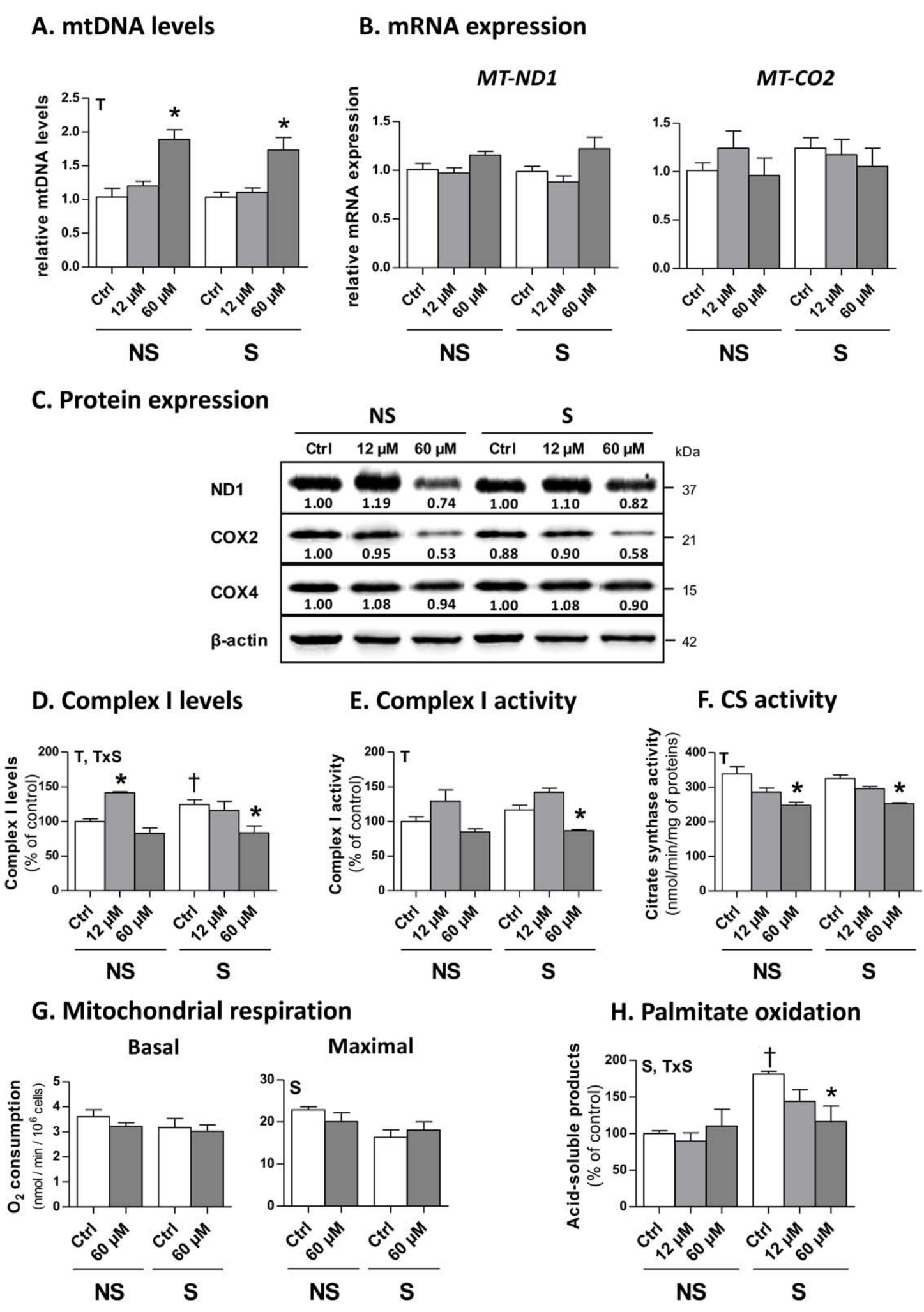

Figure 3: Mitochondrial effects of imipramine

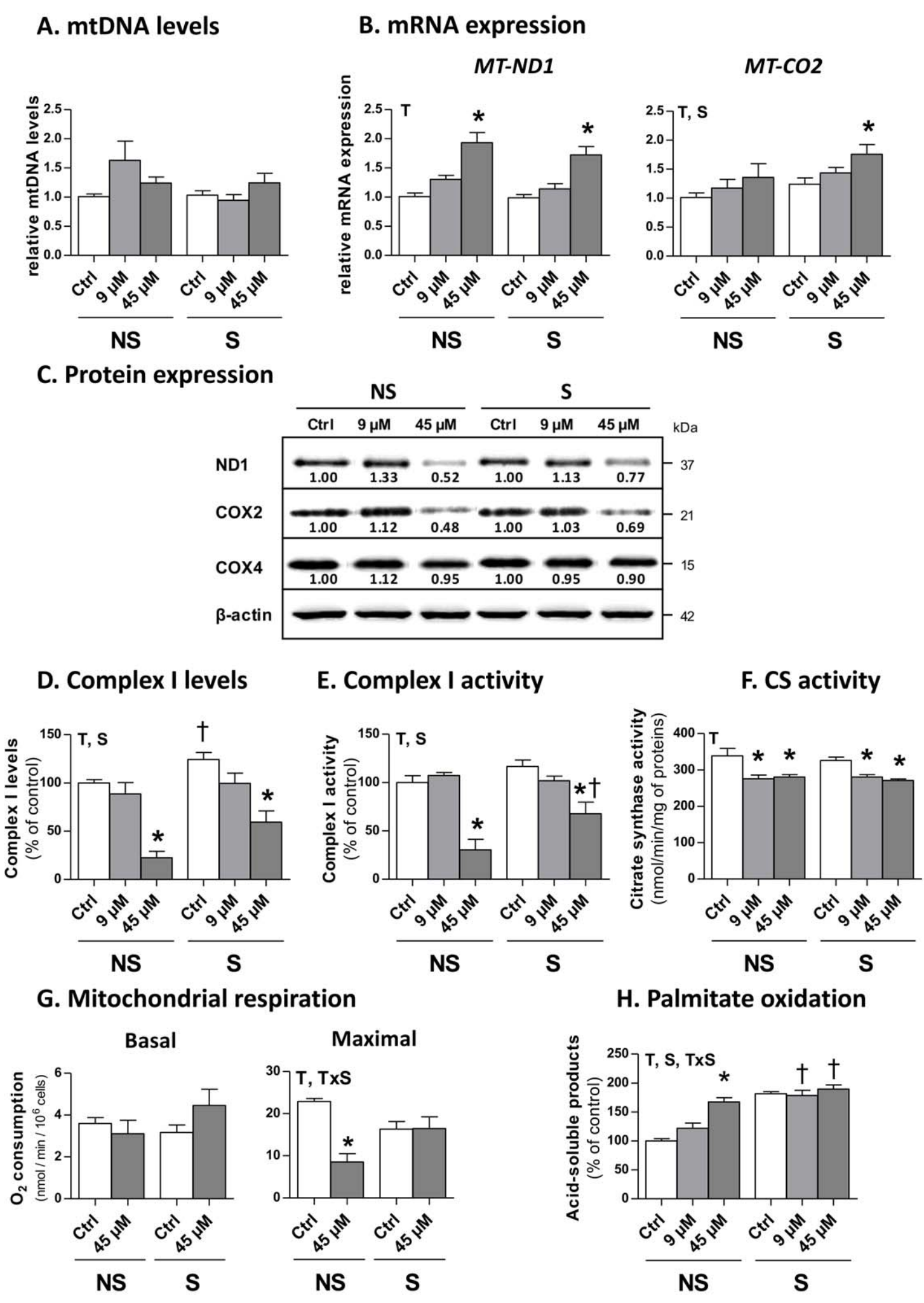

Figure 4: Mitochondrial effects of ritonavir

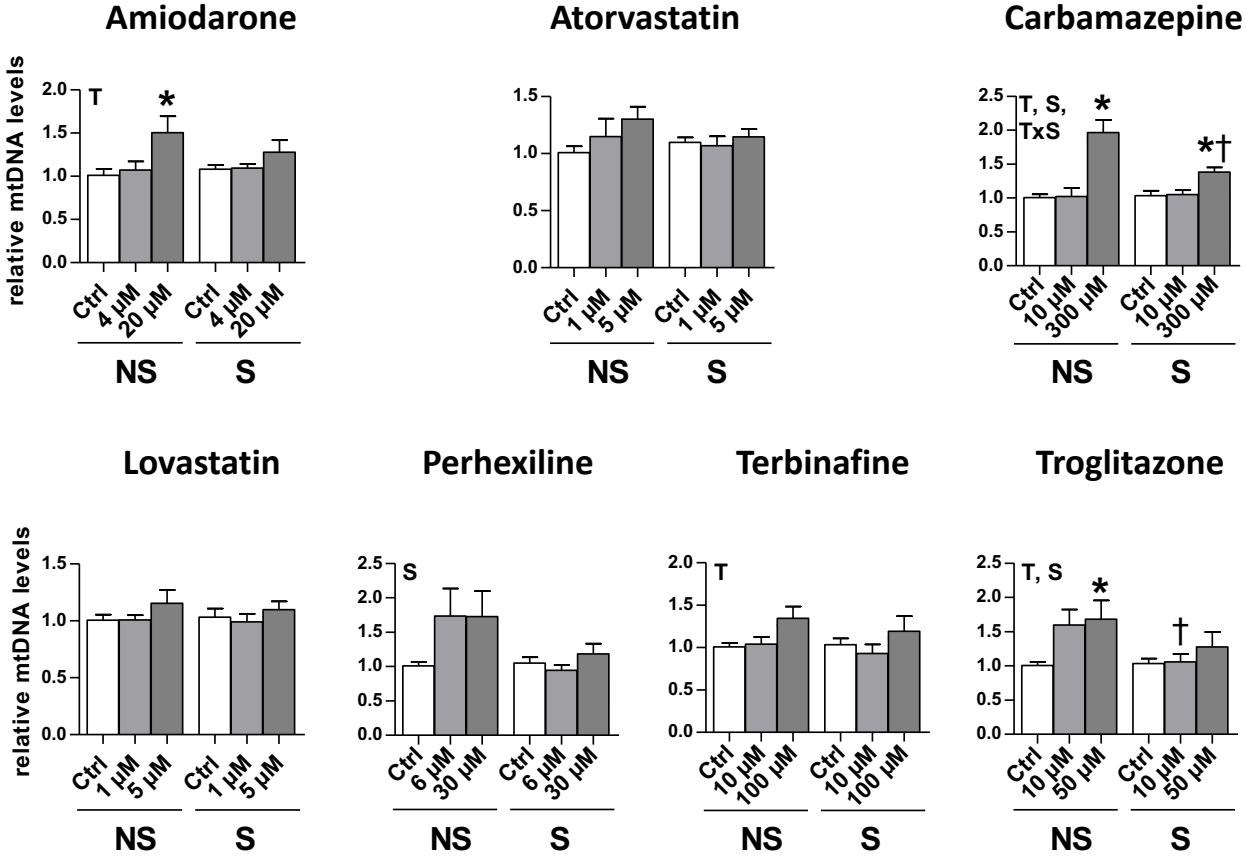

Figure 5: Drug-induced modulation of mtDNA levels

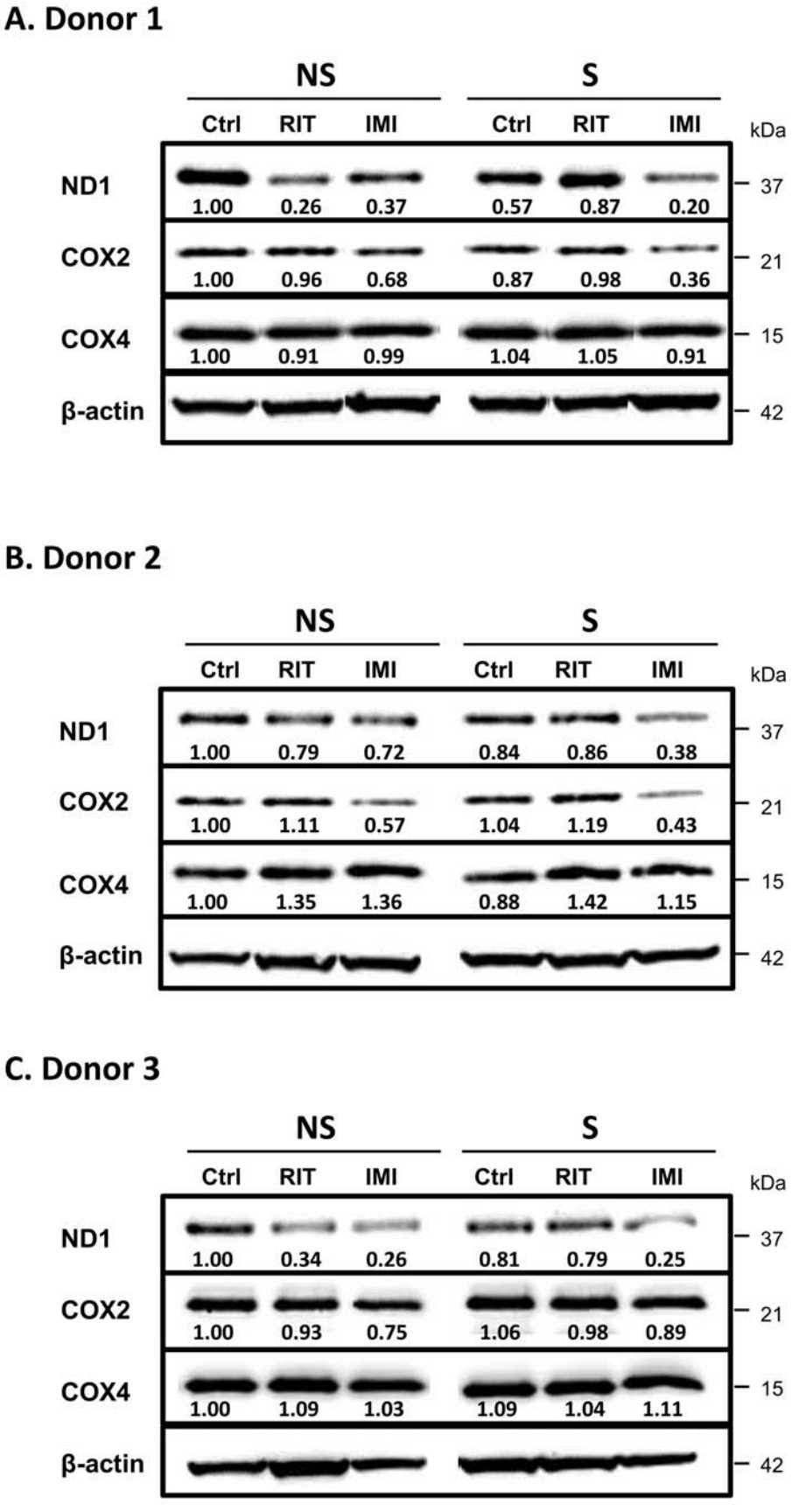

Figure 6: Effect of imipramine and ritonavir on ND1, COX2 and COX4 expression in primary human hepatocytes

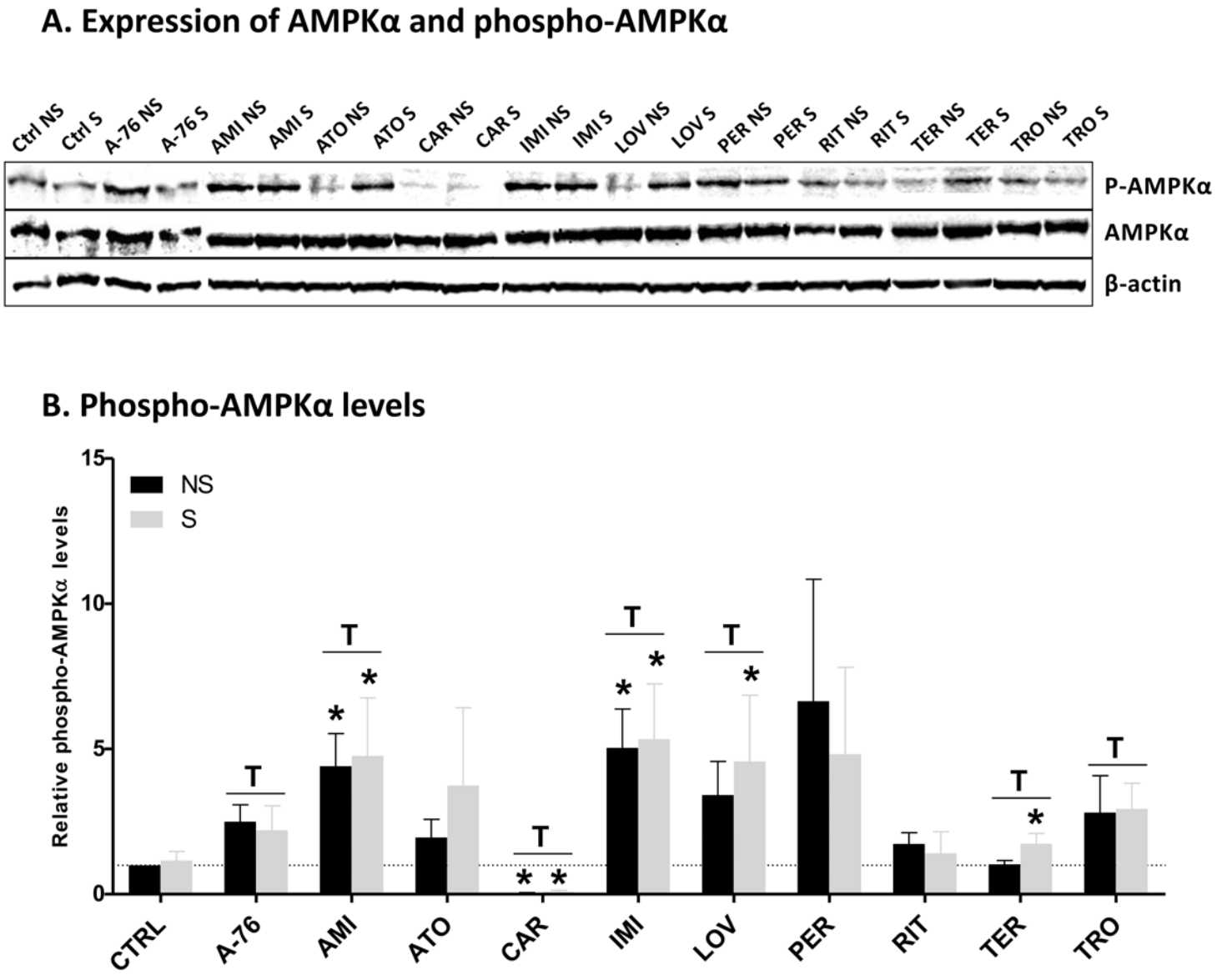

Figure 7: Drug-induced AMPK activation